University of Twente

Technical Medicine

Masterthesis

How can we reduce regional left ventricular wall stress and improve ejection fraction in heart failure patients?

Author:
Thomas Urgert BSc

Medical supervisor: Prof. J.G. Grandjean MD PhD
Technical supervisor: R. Hagmeijer PhD
Process supervisor: M. Groenier PhD
Practical supervisor: F.R. Halfwerk MD MSc

October 18, 2019

UNIVERSITY OF TWENTE.

Abstract

Introduction Heart failure with reduced Ejection Fraction (HFrEF) is a progressive disease with a low 5-year survival of <50%. Increased left ventricular wall stress in HFrEF patients is a main contributor for disease progression. Current surgical therapies for advanced symptomatic HFrEF such as assist devices or transplantation are invasive and have high morbidity. Less invasive treatments (i.e. CorCap) focus on increased end-diastolic wall stress, yet fail in the long term because of partial support only during end diastole. A possible solution is to decrease left ventricular wall stress during a full cardiac cycle. The aim of this study is to quantify regional left ventricular wall stress during a full cardiac cycle in dilated and physiological hearts. Ultimately a minimal invasive device should be developed to provide continous regional support for symptomatic HFrEF patients.

Methods Patients eligible for cardiac surgery including HFrEF patients were included in this study. Continuous 3D transesophageal echocardiography and left intraventricular pressure were obtained. Using the intraventricular pressure and principle curvature and wall thickness of local patches constructed from the ventricle regional wall stress was determined. The regional mean curvature and wall thickening were also determined. A 16-segment model of the ventricle was used to define anatomical regions. A division between patients with a physiological ventricle, heart failure patients and patients with a dilated ventricle was performed to observe differences between averaged global wall stress, curvature and sphericity. A division between patient based on ejection fraction and end-diastolic diameter was performed to compare physiological functioning hearts with HFrEF patients for regional parameters.

Results Continuous measurements were obtained in 9 patients. No significant difference in global wall stress, curvature and sphericity between patients were found. A significant difference in wall stress in the lateral wall of the ventricle was found at peak systole and end systole. Furthermore, significant differences for the lower segments of the ventricle were found at peak systole and end systole. Significant correlations between end-systolic, peak systolic, end-diastolic wall stress and cyclic variation curvature and wall thickening were found.

Conclusion Full cardiac cyclic left ventricular regional wall stress was successfully obtained during cardiac surgery. The current study provides insight into the differences in regional wall stress between physiological and impaired functioning ventricles. Regional wall stress for the middle and apical segments of the ventricle for HFrEF patients with a dilated ventricle were found to be increased at peak systole and end-systole. Correlations were found between end-systolic wall stress and peak systolic, end-diastolic wall stress and myocardial vitality.

Future research should focus on changes in regional wall stress over time after treatment and the relationship between different LVEF. Future work should develop minimal invasive devices with patient-specific full cardiac cycle support to lower the regional wall stress.

Keywords: regional wall stress, full cycle, left ventricular, heart failure, cardiac surgery

List of abbreviations

ACEi	Angiotensin-Converting Enzyme inhibitor
AMVR	Adjustable and Measurable Ventricular Restraint
ARBs	Angiotensin II Receptor Blockers
BMI	Body Mass Index
BSA	Body Surface Area
CABG	Coronary Artery Bypass Grafting
CRT	Cardiac Resynchronization Therapy
CSD	Cardiac Support Device
DCM	Dilated Cardiomyopathy
EDV	end-diastolic left ventricular Volume
EF	Ejection Fraction
ESV	end-systolic left ventricular Volume
FS	Functional Shortening
HF	Heart Failure
HFmrF	Heart Failure with midrange Ejection Fraction
HFpEF	Heart Failure with preserved Ejection Fraction
HFrecEF	Heart Failure with recovered Ejection Fraction
HFrEF	Heart Failure with reduced Ejection Fraction
LVAD	Left Ventricular Assist Device
LVEDd	Left Ventricular end-diastolic Diameter
LVEF	Left Ventricular Ejection Fraction
LVESd	Left Ventricular end-systolic Diameter
MRA	Mineralocorticoid Receptor Antagonists
QVR	Quantitative Ventricular Restraint
STL	Surface Tessellation Language
SV	Stroke Volume
TEE	Transesophageal Echocardiography

Preface

The past year could be described as a very challenging and enormously educational year for me, in which I received many opportunities to develop myself and to meet many inspiring people. For this I greatly want to thank my four supervisors. They have offered me the possibility of working together with them in this research. And next to this, they have challenged me to bring out the best of myself. Despite the fact that the current study suited the master track 'Imaging and Intervention' a bit better, compared to my master track 'Sensing and Stimulation, I have enjoyed it very much to receive the opportunity to dive into this research and learn more from several sides of Technical Medicine. I would also like to thank the Thorax Centre Twente for providing the possibility to develop myself clinically and to support my clinical ambitions. I experienced the department as a great educational place with many enthusiastic colleagues.

I hope we will cooperate again in the future!

16 October 2019
Thomas Urgert

Contents

1 Introduction

Heart Failure (HF) is a clinical progressive syndrome caused by structural and/or functional cardiac abnormality. Faulty heart valves, heart arrhythmias and genetic defects, impair pump function of the heart and cardiac output is reduced [1]. As a response to this impairment many pathways are induced to accommodate for the decrease in cardiac output to maintain normal haemodynamics. This leads to damage of the heart muscle, the myocardium. When a certain cardiac abnormality is present long enough, the myocardial muscle becomes damaged beyond reversibility. Depending on the etiology, the entire ventricle becomes enlarged and the myocardial muscle is thinned or the myocardial muscle of the ventricle becomes thickened. About 23 million people in developed countries are currently diagnosed with HF. This accounts for 1-2% of the western population [1, 2]. This prevalence will increase with 46% in 2030 due to an increase in life expectancy and cardiac problems due to an unhealthy lifestyle [3]. Heart failure is an incurable and progressive syndrome with a low 5-year survival under 50% [4]. Due to an impairment in pump function, symptoms such as dyspnoea, oedema and fatigue are characteristic for HF and lower the quality of life.

The Left Ventricular Ejection Fraction (LVEF) is used to describe the wide variety of HF patients. This LVEF is the ratio between the end-diastolic left ventricular volume (EDV) and stroke volume (SV). Differentiation by LVEF is important, because of different underlying causes, co-morbidities, treatment options and response to therapy. Physiological values are 50 to 70%. Patients with an ejection fraction <40% are considered as heart failure with reduced ejection fraction (HFrEF) patients. Patients with heart failure and a normal ejection fraction $\geq$ 50% are considered as heart failure with preserved ejection fraction (HFpEF). The 'grey area' of HF patients exists in between, with a LVEF of 40-49%, and are grouped as heart failure with midrange ejection fraction (HFmrEF). HFrEF patients are known with systolic dysfunction, whereas HFpEF patients often have diastolic dysfunction (see figure 1).

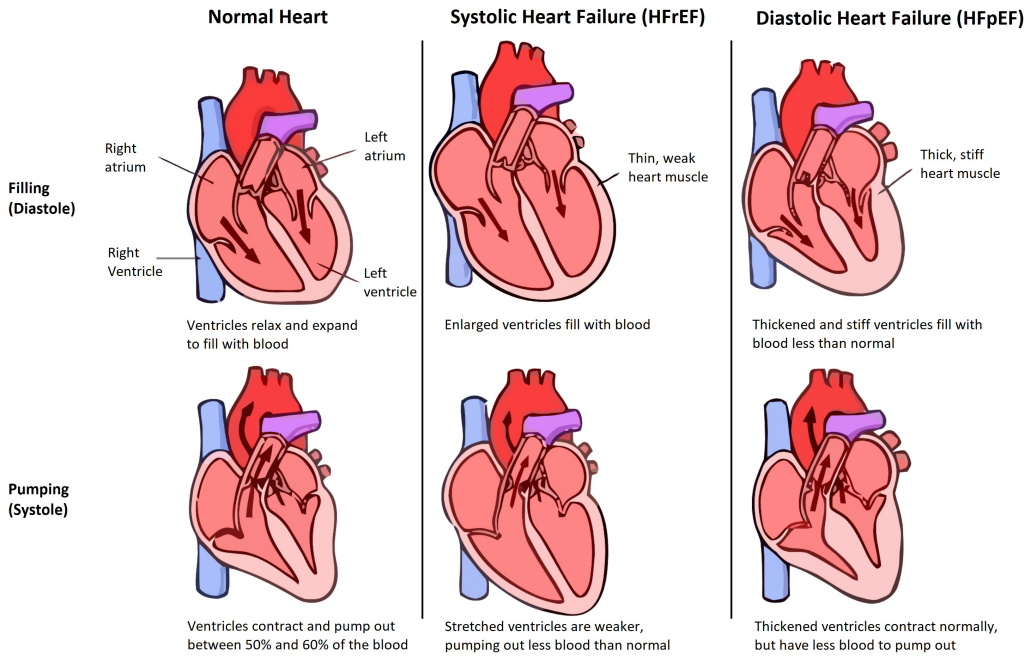

Figure 1: Representation of diastole and systole of a normal functioning, systolic dysfunctioning and diastolic dysfunctioning heart [5]

1.1 Ejection Fraction and mortality

Studies have suggested that HFpEF patients have a better survival than HFrEF patients. Studies showed an adjusted hazard ratio between 0.65-0.96 compared to HFrEF [6–10]. Thus, mortality in HFpEF patients is 0.65-0.96 of the mortality of HFrEF patients. Contradictory, some studies have shown no differences between mortality and HFrEF and HFpEF [11, 12]. When looking in depth at the mortality and LVEF a relationship becomes clear. The past decade, research has shown a decreased mortality when the LVEF is increased [9,13,14]. These studies reveal an adjusted hazard ratio compared to a LVEF of 60% for patients with a LVEF <15% of 1.75-2.5 declining to 1.10-1.25 for patients with a LVEF of 35-45% (figure 2). For every

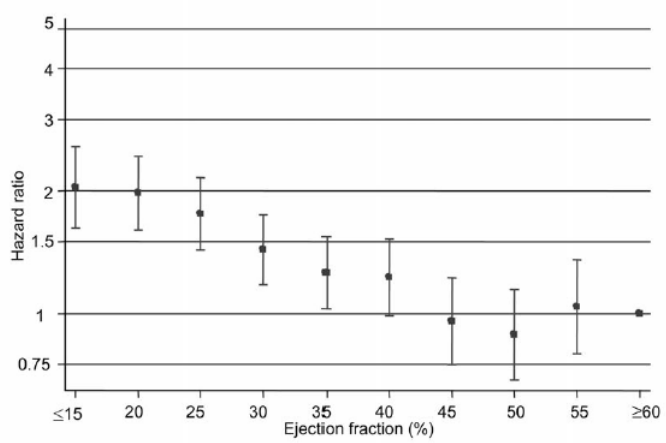

Figure 2: Relationship between LVEF and hazard ratio in heart failure patients [14]. Hazard ratio is adjusted to LVEF 60%.

5% increase in LVEF there is a 13% decrease in hazard. The mortality in patients with a LVEF >45% is not further improved when LVEF is further increased. This could be explained by the fact that the mortality of HFpEF patients is often caused by non-cardiovascular causes and that LVEF approaches normal values [1]. When an individual HFrEF patient's LVEF after treatment improves to above 45-50%, recovered LVEF (HFrecEF) results in mortality are even better. The mortality and hospitalization was lower than HFrEF, HFmrEF and HFpEF patients [15]. However, the overall mortality is still fourfold higher than healthy subjects. On top of this, a study of Lupón [16] observed an increased mortality risk when the LVEF of a patient is declining in a preceding period. Taking the above described findings into consideration, it can be hypothesized that increasing LVEF and retaining this improves the outcome of a HFrEF patient.

1.2 Current treatments

Treatments of patients with HFrEF focus on the improvement of their physiological condition, quality of life, preventing hospital (re)admission and reducing mortality [1]. Pharmacological treatment with angiotensin-converting enzyme inhibitors (ACEi), angiotensin II receptor blockers (ARBs), beta-blockers and diuretics in patients with HFrEF is recommended to reduce morbidity and mortality [1]. For patients with maintaining symptoms and a LVEF $\leq 35\%$, mineralocorticoid receptor antagonists (MRA) is beneficial for survival and reduces hospitalization. For HFmrEF and HFpEF patients studies on treatment have not shown any beneficial effects on the mortality and morbidity. Therefore, the aim for treatment of these patients is to reduce symptoms severity, treat non-cardiovascular comorbidities and improve quality of life [1].

Besides pharmacological therapy, cardiac resynchronisation therapy (CRT), has proven beneficial for survival [17]. Sudden deaths and deaths from worsening of heart failure were reduced

with CRT. Hazard ratio's after an average of 1.5 year follow-up were 0.55 for worsening of heart failure and 0.54 for sudden death with respect to treatment without CRT. Despite these positive results, CRT is only applicable in HF patients with conduction disorders and 30-40% of the treated patients remain non-responders [18].

Surgical techniques can also be used for treating patients with heart failure. For patients with heart failure based on ischemic cardiomyopathy, coronary revascularization, PCI or CABG, could be performed [19]. Beneficial effects on left ventricular function were only seen in revascularization procedures for patients with vital myocardial tissue without scarring. Patients developing mitral insufficiency, which causes additional load to the already dilated left ventricle, can undergo valve repair [19]. As left ventricular size is an important prognostic factor for survival in patients, reconstruction of the ventricle could be beneficial [19]. Such a technique for changing the geometry of the dilated left ventricle is left ventricular aneurysmectomy [19]. Patients with a local and thin-walled aneurysm are eligible for procedure. Although the above techniques have proven beneficial for reducing symptoms no reduction in mortality and hospitalization rates was seen [20].

For patients with end-stage heart the only treatment option is by receiving a heart transplant. Since the shortage of donors, a left ventricular assist device (LVAD) could be used as a bridge to transplantation or used as a destination therapy. The device comes with major downsides such as, invasiveness, the necessity of anticoagulant therapy and driveline infections.

Although there is a decrease in mortality when treating with pharmacological agents and CRT, heart failure remains a progressive disease. At a certain point pharmacological treatment is not effective anymore. Finding a new method for therapy where all HFrEF patients are eligible for treatment and progression of heart failure is further slowed down or possibly stopped is desirable.

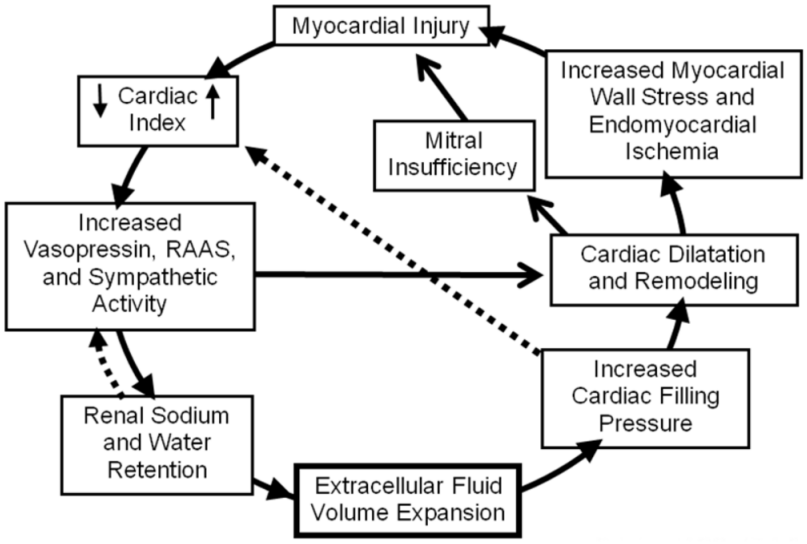

Figure 3: Vicious circle ventricular remodelling in heart failure patients [21].

1.3 Cause of progressiveness

In patients with HFrEF a dilated left ventricle, dilated cardiomyopathy (DCM) is observed (figure 1). It comes with a thinned and weakened myocardial muscle. This change in ventricular configuration is called remodelling. The general hypothesis is that many myocardial abnormalities observed in failing hearts are a direct or indirect consequence of increased myocardial wall stress and sustained neurohumoral activation [22]. Stress is defined as the force acting on a cross-sectional area. It can indirectly be determined by the relation between the

ventricular pressure, the myocardial wall thickness and curvature of the ventricle. Due to the thinning of the myocardial muscle and enlargement of the ventricle, the stress in the myocardial wall is increased. This increase in wall stress leads to an increase in oxygen demand due to the increased working load of the muscle. When this increased oxygen demand cannot be met the myocardium becomes even more damaged. This will further promote dilatation and fluid retention, which in turn causes a further increase in wall stress; entering a vicious circle (figure 3). For HFrEF patients an increase in the end-diastolic wall stress is highly associated with LV dilatation and a reduction in EF [23]. An increase in myocardial wall stress throughout the cardiac cycle will worsen the outcome. Reducing myocardial wall stress will prevent worsening of heart failure and potentially leads to reverse remodelling [24]. This would then have beneficial effects on LVEF recovery and improved survival.

1.4 Regional Wall Stress

Cardiac wall stress has found to be an important stimulus for remodelling of the left ventricle in patients with heart failure and induces hypertrophy [25–27]. It furthermore determines myocardial oxygen consumption and is of importance for the mechanical behaviour of the coronary circulation [28]. Additionally, increased wall stress adversely contribute to energy metabolism, gene expression and arrhythmia [29–31].

As described earlier, wall stress is defined as the force acting on a surface divided by the cross-sectional area over which the force acts (equation 1). Stress induced by a force acting perpendicular to a cross-sectional area is defined as the normal stress. When a force acts parallel to a cross-sectional area it is called shear stress.

$$\sigma = \frac{F}{A_w} \tag{1}$$

Definition of stress; with σ = Stress (N/m^2), F = Force (N) and A_w = Cross-sectional area of wall (m^2)

Laplace derived that the normal stress is directly proportional to the pressure inside a sphere and the radius of that sphere and indirectly proportional to the wall thickness (Appendix A). It is assumed that the material of the wall is isotropic, the sphere is in equilibrium and the wall thickness is much smaller than the radius (h<<R). This allows for treating the wall as a surface with the same material properties across the entire surface. The wall stress can be indirectly determined with:

$$\sigma = \frac{P \cdot R}{2 \cdot h} \tag{2}$$

Wall stress quantification for a sphere; with σ = Stress (N/m^2), P = Pressure (Pa), h = Wall Thickness (m), R = Radius (m)

Since the shape of the ventricle is more comparable to an ellipsoid than a sphere, the equation was further derived by using the maximum and minimum radius to determine the cross-sectional area of the ellipsoid (Appendix A). At maximum and minimum radius the bending of the surface is at maximum and minimum which can be described by the principal curvatures.

$$\sigma = \frac{P}{h \cdot (\kappa_1 + \kappa_2)} = \frac{P}{h \cdot (\frac{1}{R_1} + \frac{1}{R_2})} \tag{3}$$

Wall stress quantification for a ellipsoid; with σ = Regional Wall Stress, P = Intraventricular Pressure, h = Wall Thickness, κ_1, κ_2 = Principle Curvatures, R_1, R_2 = Radius

Using both the spherical (2) and ellipsoidal model (3) many research was conducted to assess the stress in the left ventricular wall during a cardiac cycle (table 1) [32–35]. In order to use these models, the assumption that the myocardial wall is much thinner than the radius of the ventricle was made. Furthermore, influences from the orientation of muscle fibers, stress variation across the ventricular wall and shear deformation stress are neglected. Calculations were performed at the equator of the ventricle. The location thought to be subjected to the highest wall stress, since it has the greatest radii.

Table 1: Example global wall stress for different etiologies using an ellipsoid approximation [34]

	end-diastolic Wall Stress kN/m^2	Peak systolic Wall Stress kN/m^2	end-systolic Wall Stress kN/m^2
Normal	3.2 ± 0.6	32.6 ± 2.4	12.3 ± 2.2
Mitral Stenosis	4.2 ± 0.7	35.9 ± 2.9	19.5 ± 3.4
Volume Overload	5.3 ± 0.6	35.4 ± 1.9	14.7 ± 2.0
Pressure overload compensated	3.0 ± 0.3	39.3 ± 4.3	12.2 ± 3.8

This method, however, only produces an estimate of the average or global wall stress of the ventricle. Local variations in wall stress could not be determined using this method, since the geometry of the left ventricle is more complex than an ellipsoid. Especially in patients with dilated cardiomyopathy the assumption that the ventricle is an ellipsoid is inaccurate, due to the local changes in curvature, wall thickness and contractility.

A three-dimensional (3D) regional approach is necessary to quantify the left ventricular wall stress locally. Using imaging techniques, such as magnetic resonance imaging and three-dimensional echocardiography the left ventricular can be reconstructed in 3D. By determining the curvature and wall thickness of local patches of this 3D reconstruction regional wall stresses can be determined (figure 4). Different equations were derived in order to eventually calculate regional wall stresses [35]. Despite the multiple assumptions necessary to calculate wall stresses using Laplace law it is widely accepted for quantifying regional wall stresses [35]. Assuming the local patches of the left ventricular wall to be part of a surface of an ellipsoid described by the maximum and minimum curvature (principal curvature) of that local part the regional wall stress could be calculated using equation (3) [36].

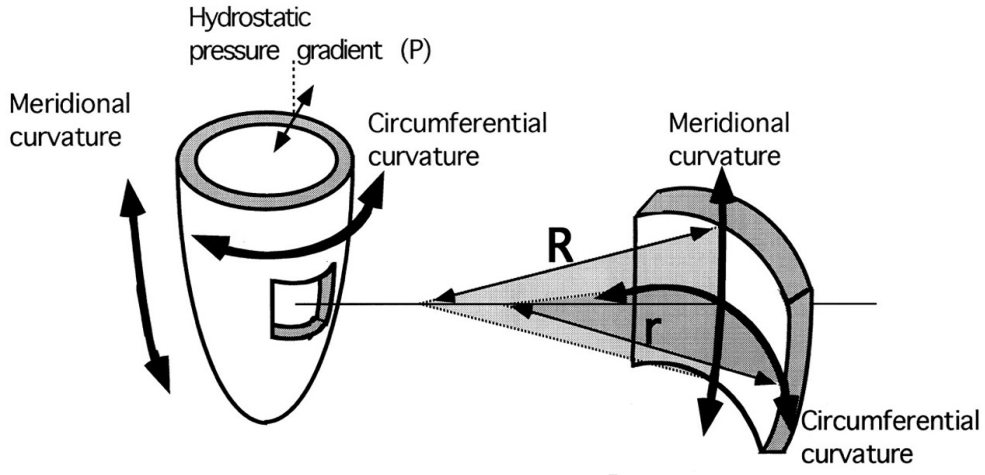

Figure 4: Schematic representation of local patch for calculating regional wall stress using Laplace's law [37]. The meriodional and circumferential curvature correspond to the principal curvature.

Research into regional wall stress is mainly performed in endsystolic and enddiastolic phase.

These studies have shown regional wall stress differences between DCM patients and subjects with a non dilated heart [27]. However regional wall stress distribution throughout a full cardiac cycle in patients is not yet researched in dept. It is thought that the level and distribution of wall stress across the entire left ventricle during the cardiac cycle have different effects on myocardial functioning and remodelling and could be another cause of the dilation of the ventricle in heart failure patients [38]. Insight would provide a quantitative evaluation of the cyclic regional wall stress and its connection to changes of the left ventricle in these patients [35]. Furthermore it provides information for the development of new treatment options for heart failure patients.

1.5 Developments in treatment options for heart failure

To tackle the issue of increased wall stress one could use restraint therapy. This is a therapy where a device superficially constrains the outsized heart. A few devices on this matter were developed, namely the CorCap cardiac support device (CSD) (CSD; Acorn Cardiovascular Inc, St Paul, Minn), Paracor HeartNet device (Paracor Medical, Sunnyvale, Calif) and the Quantitative Ventricular Restraint (QVR) device (Polyzen Inc, Apex, NC) (figure 5). The first two devices uses flexible fibers whereas the QVR uses a balloon placed around both ventricles. Results for the CorCap and HeartNet showed improvement in symptoms, physical well-being and quality of life. Furthermore, reverse remodelling had occurred.

Despite positive early outcomes, no increase in survival was found [39, 40]. This could be explained by the lack of adjustable and measurable ventricular restraint (AMVR) by the device and that the device only acts at end diastole [40]. Once reverse remodelling occurs and the heart is reconfigured the device should adapt to this new configuration will it provide further restraint. A device which is able to AMVR is the QVR. In ovine models AMVR showed a promising increase in LVEF of around 19 % and a decrease in EDV of 12%. The same study showed that AMVR is more effective than nonadjustable restraint in the promoting of reverse remodelling, increase in LVEF and decrease in EDV [41]. Downside of the device is the necessity of per-cutaneous leads to measure and adjust the filling of the balloon. Besides, differences in regional reduction in wall stress cannot be obtained using this device and it lacks support throughout the cardiac cycle. Another study concluded that restraint only applied on the left ventricle may be more effective than standard restraint [42]. Finding a restraint device which can adjust and measure the ventricular restraint and apply different support regionally throughout the cardiac cycle could be beneficial for the survival of HFrEF patients.

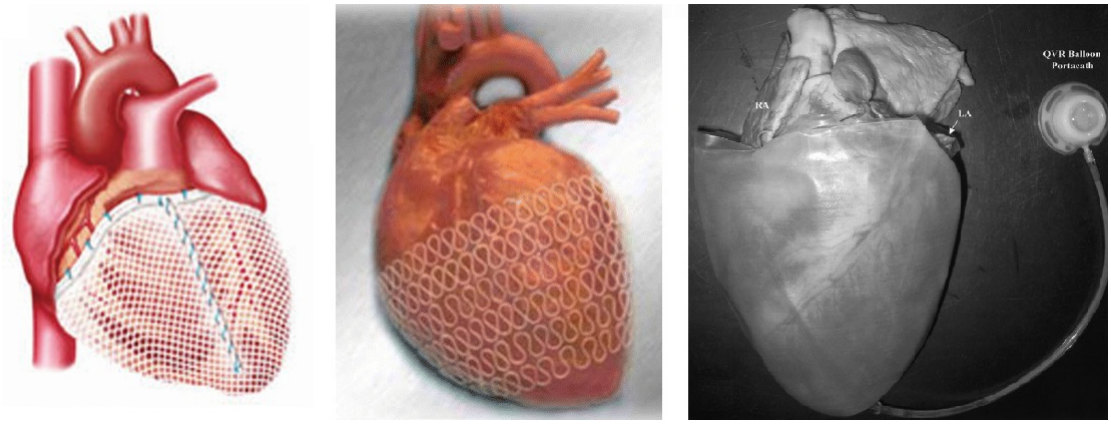

Figure 5: Left: CorCap, Middle: HeartNet, Right: QVR [40, 43, 44]

1.6 Objective

The aim of this study is to investigate regional full cardiac cycle wall stresses of the left ventricle. The secondary aim is to find a possible way to gradually reduce and maintain wall stress over time, to guide reverse remodelling and therefore increasing the ejection fraction in patients with HFrEF.

The following questions are central in this study:

- What are the regional wall stresses across the left ventricle throughout the cardiac cycle for healthy subjects and heart failure patients with different etiologies?
- What is the optimal device configuration for externally reducing the wall stress and increasing the ejection fraction?

2 Methods

2.1 Study design

This explorational case–control pilot study comprised of quantifying the full cardiac cycle regional myocardial wall stress in vivo of patients who were undergoing surgery. Quantification of regional wall stress was performed in patients with a physiological functioning left ventricle and heart failure patients. After median sternotomy and before the actual intervention measurement of the three-dimensional geometry of the left ventricle using transesophageal echocardiography (TEE) and simultaneous measurement of the left ventricular pressure were performed. With this the regional wall stress and relevant parameters were determined using an in-house developed algorithm.

2.2 Setting

The study was conducted at the department of Cardiothoracic surgery at the Thorax Centre Twente at the Medical Spectre Twente Hospital, the Netherlands. After approval by the Medical Ethical Committee (K19-24) patients were included the period between 11-04-2019 until 17-09-2019.

2.3 Participants

It was aimed to include 10 patients. The protocol was amended on 29-08-2019 to include patients with a BMI over 30 kg/m^2 and total number of patients was increased to 18. Patients with a dilated left ventricle and/or decreased pump function and subjects with a normal function and non dilated left ventricle were eligible for enrolment. A decreased pump function was defined as LVEF<40%. Patients with a left ventricular end-diastolic diameter (LVEDd) higher than 52mm where defined as patients with a dilated left ventricle. Patients undergoing Coronary Artery Bypass Grafting (CABG), Aortic- or mitral valve replacement or repair and patients undergoing aneurysmectomy were eligible for inclusion. Exclusion was performed when patients had a body mass index (BMI) of more than $39kg/m^2$ or when patients mental well being did not allow for inclusion. Patients of one surgeon were measured after giving written informed consent.

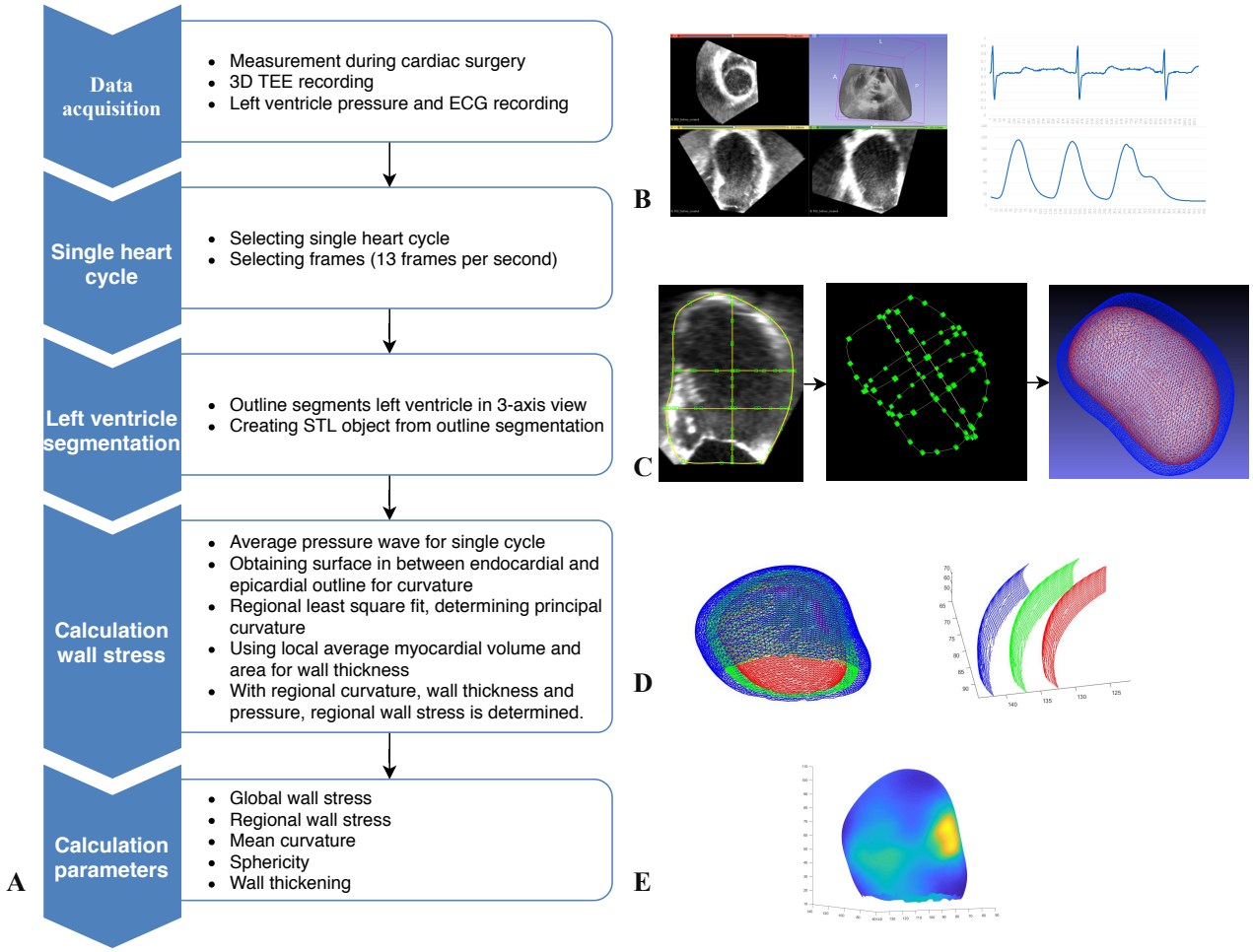

Figure 6: Schematic representation of the algorithm used to obtain full cycle regional wall stress. A) Flow chart of methods; B) per-operative TEE of left ventricle and per-operative intraventricular pressure; C) contouring left ventricle and creating surface tessellation language; D) obtaining surface in between (green) epicardial (blue) and endocaridal contour (red); E) regional wall stress across left ventricle.

2.4 Data acquisition

The Philips EPIQ 7C ultrasound system (Philips Medical Systems, the Netherlands) was used to acquire the three-dimensional geometry of the left ventricle. Using the transesophageal echocardiography probe the heart was visualised in 2D from the 4-chamber point of view. Using the 3D mode and 3D zoom the entire left ventricle was made visible and was captured. The build-in software averaged automatically multiple heart cycles into one heart cycle, based on the R-wave of the ECG signal, to improve image quality. In time multiple of these recordings were made and saved. Afterwards, the best quality recording was used to obtain the geometry. One heart cycle consisted of about 15 to 30 frames depending of the heart rate. The echocardiographic data was exported from the Philips Intellispace database as a DICOM format.

An arterial catheter (Arrow® International Inc.) for left ventricle venting was inserted just before the measurements. Simultaneously with the TEE recordings, the left ventricular pressure was captured using a Philips Intellivue MP70 monitor (Philips Medical Systems, the Netherlands) and free available Vital Signs capture (Xeonfusion) software. The pressure was captured with a sample frequency of 128 Hz. Together with the pressure measurements the

ECG-signal was recorded by the monitor at 512 Hz. This was performed in order to be able to match the TEE and pressure recordings for the exact time.

2.5 Data analysis

Data analysis was performed in four steps. These steps are represented in figure 6. After the data was acquired, first, one full heart cycle of the TEE data was determined and processed. From the echographic data of a single heart cycle the myocardium of the left ventricle was segmented. With the segmented left ventricle and pressure data the wall stress was then calculated. Additionally extra parameters described in section 2.5.4 were determined.

2.5.1 Single heart cycle

Using 3D Slicer 4, a free and open source scientific software package, one heart cycle from the echographic data was determined. The frame with the closing of the mitral, end-diastole, was chosen as the beginning of the heart cycle. The frame just before closing of the mitral valve, after systole, was chosen as the last frame for the cardiac cycle. One heart cycle was then subdivided to decrease the amount of data to manually process later. It was thought that choosing 13 frames per second was sufficient to capture the motion of the ventricle during a full cardiac cycle. Practically, it meant that a heart cycle recording of for example 20 frames was divided into 10 single frames. These single frames, containing the 3D data at that certain moment in time, were exported and saved.

2.5.2 Left ventricle segmentation

In MeVisLab (MeVis Medical Solutions AG, Fraunhofer MEVIS, Germany) an algorithm was created in order to trace the endocardial and epicardial contour of the left ventricle (figure 6.C). The endocardial contour represents the inside contour of the myocardium where the epicardial contour represents the outside contour of the myocardium. Tracing the contours in the selected frames of the heart cycle was performed by manually placing seed points in the long and short axis views. Using the built-in spline surface function for interpolation between points the whole ventricle was segmented. Visually checking and adjusting was performed to make sure the interpolation followed the exact contour. The traced contour was then transformed into a surface tessellation language (STL) object using the programs recursive marching-cubes algorithm. A STL object is a triangular representation of a 3-dimensional surface geometry. The created STL-objects were smoothed in order to diminish minor irregularities of the surface created by the marching-cubes algorithm. Smoothing was performed using a build-in Laplacian smoothing filter in MeshLab (ISTI-CNR, Italy). The final 3D segmented left ventricle was created by cutting the STL-object at the height of the annulus of the mitral valve.

2.5.3 Calculation wall stress

The final 3D segmentations and pressure recordings were analyzed using an in-house written algorithm in MATLAB R2018b (MathWorks, Natick, MA, USA). This in-house written algorithm was based on the article by Oomen et al. (1999) [36] for analyzing regional wall stress in echographic imaging. With the pressure, wall thickness and curvature during a full cardiac cycle, the regional wall stresses were determined.

Pressure The left ventricle pressure recordings at the time of TEE recording were loaded and automatically averaged over 6 heart beats using the R-wave of the ECG. Averaging the pressure wave over 6 heart beats was preformed since the TEE-recording was averaged over

6 heart beats as well. Using the R-wave the beginning of the heart cycle was marked and the pressure curve was matched in time with the TEE recording. The right pressure points matching the time of the segmented echocardiographic frames were then determined.

Wall thickness The wall thickness was determined for all vertices of the STL-object of the endocardial contour. First, the outward pointing normal of each vertex was determined. The location of the vertex and the direction of the normal vector was used to construct a vector which intersect the epicardial contour. The wall thickness for a particular vertex was eventually determined with the magnitude of the vector at the point of intersection with the epicardial contour.

Curvature In order to calculate the curvature of the mycocardium, a surface in between the endocardial and epicardial contour, mid-surface, was determined (figure 6.D). This was performed in order to capture the average curvature of the myocardial wall. The mid-surface was constructed with location and direction of the normal vector of each vertex. Half of the magnitude of that vector intersecting the epicardial contour was defined as the middle. Secondly, a cut-out patch of 6 layers of triangles around each vertex of the entire ventricle, approximately 4 cm wide, was created. Each cut-out was first rotated so that the normal of the vertex becomes [-1 0 0]. With that the data can be described using [X] and [Y] instead of [X], [Y] and [Z]. On the rotated cut-out a least squares patch ($f(x, y) = ax^2+by^2+cxy+dx+ey+f$) was fitted. Using the eigenvalues of the Hessian-matrix of the least square patch, the two principle curvatures of each patch were eventually determined.

Wall stress The calculation of the regional wall stress was performed with the equation (3):

$$\sigma = \frac{P}{h \cdot (\kappa_1 + \kappa_2)}$$

σ = regional wall stress, P = intraventricular pressure, h = wall thickness, κ_1, κ_2 = principle curvatures

For each patch around each vertex the wall stress was calculated using the principle curvature and wall thickness of that patch. The average of the wall thickness at each vertex in the local patch was used as the final wall thickness for that patch. The calculation of regional wall stress was performed for every segmented frame of the cardiac cycle to obtain the full cardiac cycle regional wall stress.

2.5.4 Calculation parameters

The above determined regional wall stresses were used for the calculation of global wall stress and average wall stresses in the anterior, lateral and inferior wall of the ventricle. The global wall stress was determined in order to compare the wall stress during a cardiac cycle for different patients globally. The average wall stress at the three outside walls of the ventricle was calculated to observe effects in change in pump function and ventricular shape in the three walls. The global wall stress and wall stress per wall was determined by averaging the previous calculated regional wall stress according to their location. A 16-segment model as defined by the American society of echocardiography [45] (figure 7) was used to observe for differences in regional wall stress, curvature and wall thickness between patients for a full cardiac cycle. A global curvature, curvature of the anterior, lateral and inferior wall and curvature for each of the 16-segments were also determined. First, the mean of the principal curvatures were calculated. Then the average curvature was calculated as followed: $Curvature = \sqrt{\frac{\kappa_1+\kappa_2}{2}}$. The sphericity

of the ventricle was also calculated. It is defined as the volume divided by the length of the ventricle: $Sphericity = \frac{LV_{volume}}{LV_{length}}$.

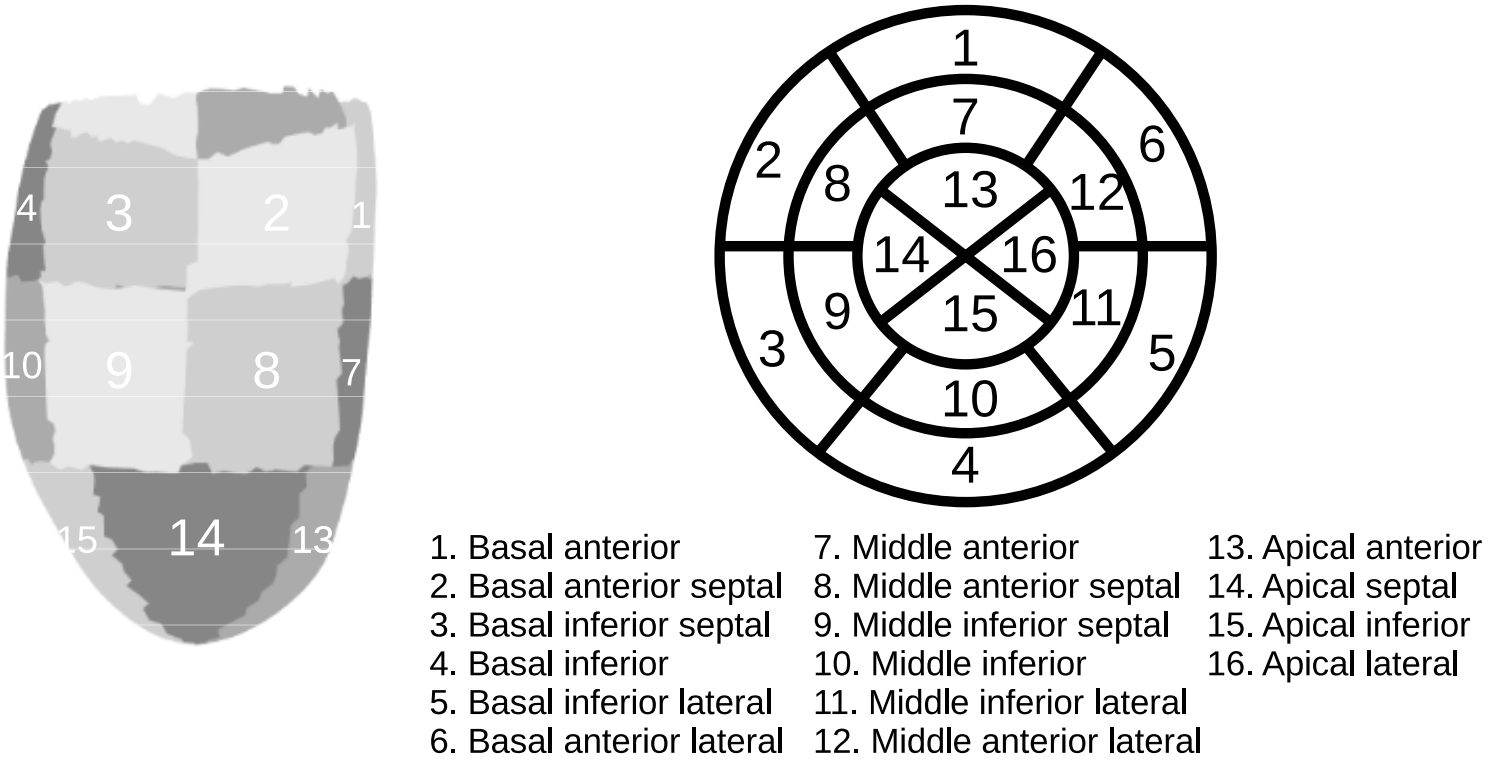

Figure 7: 16 segments left ventricle location characterisation

2.6 Statistical analysis

The overall wall stress, median curvature and median sphericity of the left ventricle was compared using a a Mann-Whitney U test between patients with a physiological functioning ventricle, patients with an impaired pump function, patients with a mid-range pump function and patients with a dilated ventricle and impaired pump function. This division was based on the left ventricular ejection fraction and left ventricular end-diastolic diameter.

Using only the left ventricular ejection fraction two groups of patients were defined for the analysis of regional wall stresses. A physiological group was defined with a EF $> 45\%$ and a HFrEF group was defined with a EF $< 45\%$. A second division of patients into two groups was based on the left ventricular end-diastolic diameter. Patients with a LVEDd higher than 52mm were classified as patients with an dilated ventricle [46]. A Mann-Whitney U test was used, since the study population is small and data was not normally distributed, to compare regional wall stress between the physiological and HFrEF group and between the physiological and dilated ventricle group. With Spearman's rho, correlations between the regional deformation of the myocardial wall, i.e. change in curvature and wall thickness during the cardiac cycle, and regional wall stress was calculated to observe for a relation between wall stress and myocardial viability. Values were presented as the median and 25-75 percentile interquartile range. When a group consisted of only two patients, the median and maximum and minimum values were presented.

Besides the author, two additional observer performed the contouring and segmentation of the left ventricle during a single heart cycle of one patient. Thereafter, an intraclass correlation (ICC) was performed to observe the interobserver reliability for the calculated wall stress across the 16-segments of the ventricle during a cardiac cycle. One observer performed contouring of

the left ventricle of one patient two times in two different days. Again an ICC was conducted to asses the intraobserver reliability. IBM SPSS statistics 25 (IBM, New York, NY, USA) was used for the statistical analysis.

3 Results

In total 11 patients were included in the study. Four patients had a normal systolic functioning left ventricle, two a dilated left ventricle with an impaired pump function, two patients had an impaired pump function with normal left ventricle dimensions and one patient had a mid range impaired pump function with normal left ventricle dimensions. Two patients were excluded from analysis. For one of the two patients, measurement of the left ventricle pressure during surgery failed. For the other patient the left ventricle was not captured entirely by the TEE. Thus in total 9 patients were eligible for analysis. Median age was 73 (IQR = 69-74). Median ejection fraction for patients with normal systolic function was 63% (IQR = 57-70%), for patients with a dilated ventricle EF was 32.5% (32-33%) and for patients with an impaired pump function, but with normal left ventricle dimensions the EF was 35% (34-36%). Other patients characteristics are shown in table 2.

3.1 Full Cycle Regional Wall Stress

Wall stresses during a full cardiac cycle was obtained successfully. Figure 8 shows an example of regional differences during a full cardiac cycle.

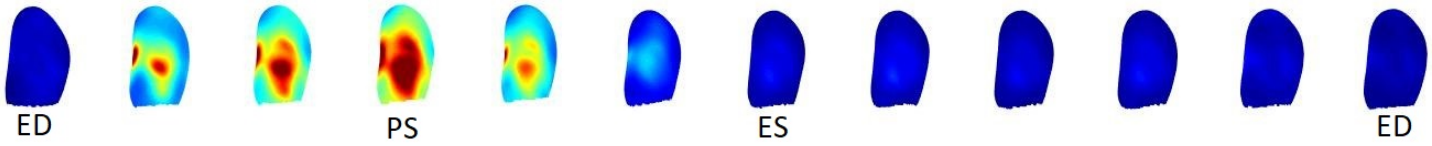

Figure 8: Example regional wall stresses during a full cardiac cycle; ED = end diastole, PS = peak systole and ES = end systole.

3.2 Global parameters

First, global parameters, containing the mean wall stress, mean curvature and mean sphericity across the left ventricle were calculated to perform a global comparison between patients. The overall wall stresses across the left ventricle during one cardiac cycle for all patients is shown in figure 9.

Table 2: Patient characteristics

Patient	Gender	Age [y]	Weight [kg]	Length [cm]	BMI [kg/m^2]	BSA [m^2]	LVEF [%]	EDV [mL]	ESV [mL]	LVEDd [mm]	LVESd [mm]	FS [%]	Surgery
1	Male	74	76	172	25.6	1.91	56	84	37	37	24	35	CABG+AVR+Bentall
2	Male	74	75	176	24.2	1.91	61	125	48	39	26	33	CABG
3	Male	71	97	168	34.4	2.13	34	136	93	54	45	16	CABG+AVR
4	Male	73	63	171	21.5	1.73	32	247	167	65	54	17	CABG
5	Male	67	72	172	24.3	1.85	36	109	70	45	39	14	AVR
6	Female	81	51	163	19.2	1.52	48	70	36	45	34	25	CABG
7	Male	73	89	168	31.5	2.04	65	51	18	40	28	30	CABG+AVR
8	Female	74	67	162	25.5	1.74	71	92	27	52	32	39	CABG+MVP
9	Male	66	103	175	33.6	2.24	33	266	180	61	52	14	CABG+MVP

BMI: body mass index, BSA: body surface area, LVEF: left ventricular ejection fraction, EDV: end diastolic volume, ESV: end systolic volume
LVEDd: left ventricular end diastolic diameter: LVESd: left ventricular end systolic diameter, FS: functional shortening

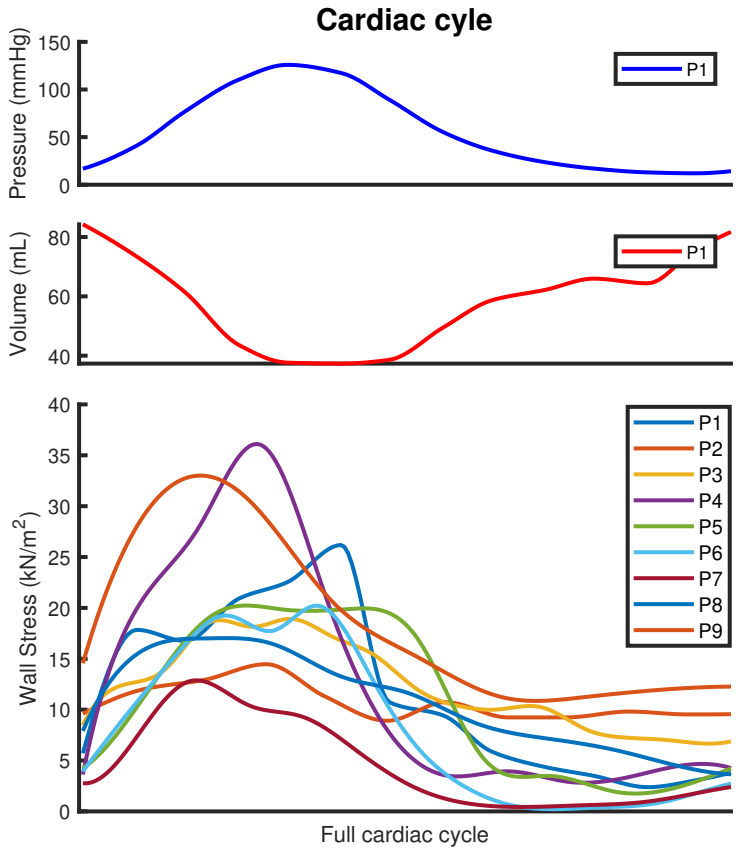

Figure 9: Overall wall stress of all 9 patients during cardiac cycle for different ventricle function and dimension. Upper: example ventricular pressure during a cardiac cycle (P1). Middle: example ventricular volume during a cardiac cycle (P1)

For a general comparison, a differentiation in patients based on ejection fraction and end-diastolic diameter according clinical measures, was performed. Four different groups were defined: physiological, HFmrEF, HFrEF and dilated HFrEF. The overall wall stresses across the left ventricle during one cardiac cycle for these four groups can be observed in figure 10.

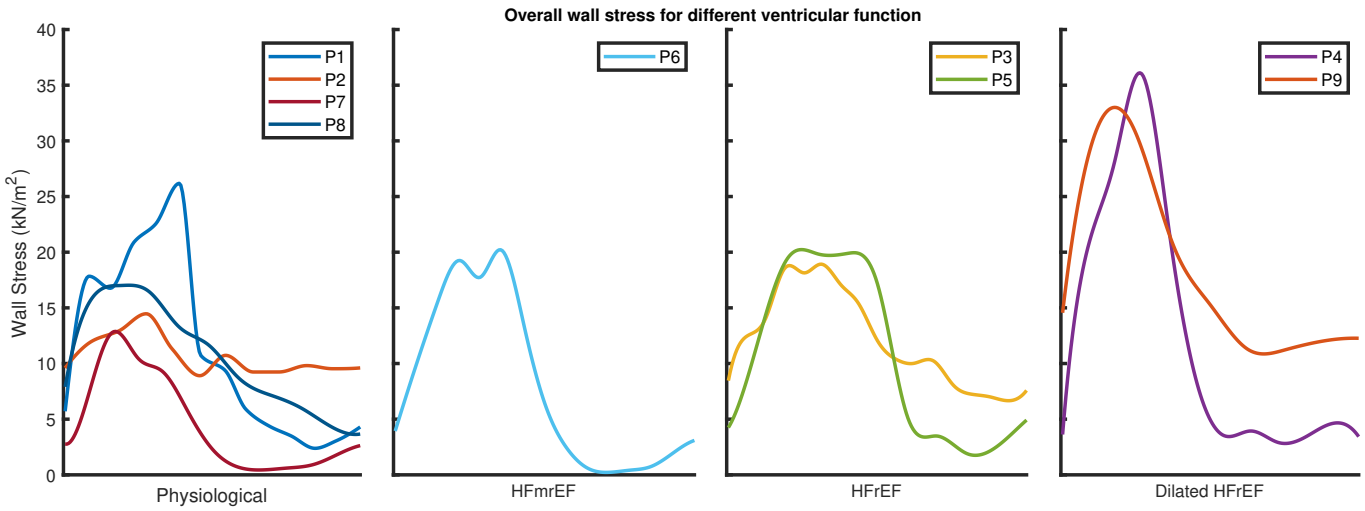

Figure 10: Overall wall stress during cardiac cycle for all 9 patients for different ventricle function and dimension.

For ease of comparison between overall wall stress, curvature and sphericity three points in time were determined: end diastole, peak systole and end systole. Table 3 shows overall wall stress in time. A Mann-Whitney U test showed no significant difference ($p > 0.05$) in overall wall stress for each moment in time between the physiological group and HFmrEF, HFrEF and dilated HFrEF groups. The corresponding p-values are shown in table 14 in Appendix B.

Table 3: Overall wall stress during cardiac cycle

	Physiological		HFmrEF	HFrEF		Dilated HFrEF	
WS_{ED} [kN/m^2]	6.8	[3.5-9.2]	3.9	6.4	[4.2-8.5]	9.1	[3.6-14.6]
WS_{peak} [kN/m^2]	17.6	[13.2-23.9]	20.2	19.4	[18.9-19.9]	33.7	[31.5-36.0]
WS_{ES} [kN/m^2]	11.0	[7.0-11.6]	6.4	8.7	[5.3-12.0]	21.5	[20.6-22.3]

WS: wall stress, ED: end-diastolic, peak: peak systolic, ES: end-systolic

The overall curvature values for the four patients groups is shown in table 4. The percentage in difference between end-diastolic overall curvature and end-systolic overall curvature was calculated for a measure of the ventricles ability to change shape during a contraction. Using a Mann-Whitney U test, no significant difference ($p > 0.05$) in overall curvature was found between the four groups, see table 14. Furthermore, no significant difference ($p > 0.05$) was found between the percentage in change of curvature across the groups, see table 14.

Table 4: Overall curvature during cardiac cycle

	Physiological	HFmrEF	HFrEF	Dilated HFrEF
Curvature_{ED} [mm^{-1}]	0.037 [0.035-0.049]	0.037	0.029 [0.028-0.030]	0.027 [0.026-0.028]
Curvature_{peak} [mm^{-1}]	0.047 [0.038-0.061]	0.045	0.032 [0.030-0.034]	0.029 [0.029-0.029]
Curvature_{ES} [mm^{-1}]	0.052 [0.040-0.071]	0.045	0.032 [0.030-0.034]	0.029 [0.029-0.030]
ΔCurvature [%]	27% [13-44%]	23%	10% [9-12%]	10% [8-11%]

ED: end-diastolic, peak: peak systolic, ES: end-systolic

The ventricular volume was divided by the length of the ventricular long axis in order to be able to compare the degree of sphericity between the four groups of patients. These values are shown in table 5. No significant difference ($p > 0.05$) in sphericity was found between the four groups, see table 14. Furthermore, no significant difference ($p > 0.05$) was found between the percentage in change in sohericity across the groups, see table 14.

Table 5: Overall sphericity during cardiac cycle

	Physiological	HFmrEF	HFrEF	Dilated HFrEF
Sphericity_{ED} [ml/mm]	1.1 [0.7-1.3]	0.9	1.4 [1.3-1.5]	2.5 [2.5-2.5]
Sphericity_{peak} [ml/mm]	0.6 [0.4-0.9]	0.6	1.0 [0.9-1.1]	2.0 [1.8-2.2]
Sphericity_{ES} [ml/mm]	0.5 [0.3-0.7]	0.6	1.0 [0.9-1.1]	1.8 [1.8-1.8]
ΔDelta Sphericity [%]	52% [43-60%]	40%	27% [22-32%]	29% [27-31%]

ED: end-diastolic, peak: peak systolic, ES: end-systolic

3.3 Cyclic differentiation between ventricular outside segments

Average wall stresses across the anterior, lateral and inferior wall of the left ventricle were determined to observe which walls would be effected by a change in pump function and ventricular shape. An example for the wall stress between anterior, lateral and inferior wall of the left ventricle for two patients is shown in figure 11.

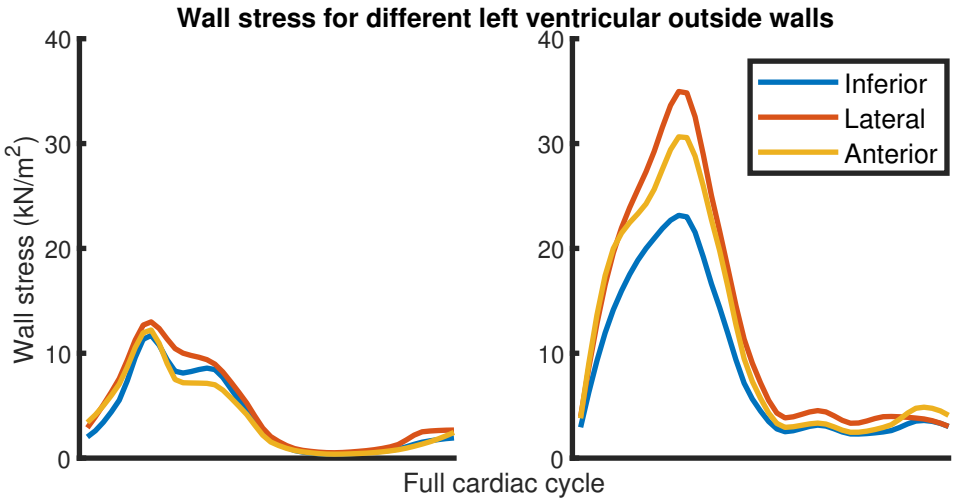

Figure 11: Wall stress across outside walls left ventricle; Left: example physiological functioning left ventricle (P7), Right: dilated HFrEF left ventricle (P4).

Comparisons between two patients groups according the LVEF (EF > 45% and EF < 45%) and LVEDd (LVEDd < 52mm, LVEDd > 52mm) were made. The wall stress based on grouping for EF for each different outside wall at end diastole, peak systole and end systole are shown in table 6. A significant difference (U = 0.00, Z = -2.45, p = 0.01) in peak systolic wall stress for the lateral wall between patients grouped for LVEF was found. For patients grouped according there LVEDd, a significant difference (U = 1.00, Z = -2.07, p = 0.04) for the lateral wall at peak systole was found. Furthermore a significant difference for the inferior wall (U = 1.00, Z = -2.07, p = 0.04) and lateral wall (U = 0.00, Z = -2.32, p = 0.02) at end-systolic was found. All p-values for the comparison based on LVEDd can be found in table 15 in Appendix B.

Table 6: Wall stress per outside left ventricular wall during cardiac cycle based on LVEF differentiation

		Physiological (EF >45%) n = 5		HFrEF (EF <45%) n = 4		p-value
WS_{ED} [kN/m^2]	Inferior	3.6	[2.2-6.6]	5.9	[3.2-9.2]	0.33
	Lateral	2.9	[2.7-7.1]	5.6	[3.9-12.5]	0.22
	Anterior	3.8	[3.2-8.9]	5.7	[3.8-9.2]	0.46
WS_{peak} [kN/m^2]	Inferior	12.5	[11.6-15.9]	18.1	[12.7-22.1]	0.22
	Lateral	13.0	[10.9-13.7]	23.3	[14.3-34.1]	0.01
	Anterior	13.1	[12.3-17.1]	19.6	[15.8-28.4]	0.09
WS_{ES} [kN/m^2]	Inferior	7.7	[5.6-9.9]	11.0	[6.2-14.7]	0.22
	Lateral	7.9	[5.4-8.8]	14.5	[6.1-21.6]	0.22
	Anterior	9.2	[5.3-11.8]	12.0	[7.2-18.7]	0.33

WS: wall stress, ED: end-diastolic, peak: peak systolic, ES: end-systolic

Also the same comparison was performed for the curvature for each outside wall. The results for comparison on curvature for the two groups based on LVEF are shown in table 7. When grouped based on LVEDd a significant difference in curvature of the inferior and lateral wall were found at peak and end systole. Furthermore, a significant difference in curvature of the inferior wall at peak systole and a significant difference in curvature of inferior, lateral and anterior wall at end systole were found.

Table 7: Curvature per outside left ventricular wall during cardiac cycle based on LVEF differentiation

		Physiological (EF >45%) n = 5		HFrEF (EF <45%) n = 4		p-value
Curvature$_{ED}$ [mm^{-1}]	Inferior	0.035	[0.034-0.048]	0.027	[0.025-0.029]	0.01
	Lateral	0.034	[0.031-0.044]	0.027	[0.025-0.028]	0.01
	Anterior	0.040	[0.036-0.045]	0.030	[0.023-0.035]	0.05
Curvature$_{peak}$ [mm^{-1}]	Inferior	0.041	[0.039-0.065]	0.028	[0.025-0.032]	0.01
	Lateral	0.040	[0.034-0.058]	0.029	[0.027-0.031]	0.05
	Anterior	0.047	[0.042-0.065]	0.033	[0.027-0.041]	0.03
Curvature$_{ES}$ [mm^{-1}]	Inferior	0.046	[0.043-0.068]	0.029	[0.026-0.032]	0.01
	Lateral	0.046	[0.034-0.066]	0.030	[0.028-0.031]	0.01
	Anterior	0.050	[0.048-0.069]	0.035	[0.028-0.044]	0.01

ED: end-diastolic, peak: peak systolic, ES: end-systolic

To observe for cyclic variation in wall stress and curvature for each outside wall based on the differentiation on ejection fraction, the standard deviation in time was calculated (see table 8, 9). Comparison for the variation in wall stress and curvature based on LVEDd can be found in table 16 in the Appendix B. No significant difference was found for the variation in wall stress in systole and diastole between the groups based on LVEF and LVEDd. The variation in curvature was significantly different during systole and diastole between the two groups. With a higher variation in curvature for the patients with a physiological functioning ventricle.

Table 8: Variation in wall stress per outside left ventricular wall during systole and diastole based on LVEF differentiation

		Physiological (EF >45%) n = 5		HFrEF (EF <45%) n = 4		p-value
Variation WS$_{systole}$ [kN/m^2]	Inferior	4.7	[3.0-5.9]	6.1	[2.7-7.3]	0.46
	Lateral	3.6	[3.1-4.4]	7.1	[3.3-10.8]	1.00
	Anterior	5.2	[2.5-6.1]	6.2	[3.7-9.2]	0.46
Variation WS$_{diastole}$ [kN/m^2]	Inferior	2.0	[0.7-3.5]	1.1	[0.8-1.3]	0.46
	Lateral	1.9	[0.9-3.3]	1.6	[1.1-2.2]	0.22
	Anterior	2.7	[0.9-4.2]	1.2	[1.0-1.7]	0.22

WS: wall stress

Table 9: Variation in curvature per outside left ventricular wall during systole and diastole based on LVEF differentiation

		Physiological (EF >45%) n = 5		HFrEF (EF <45%) n = 4		p-value
Variation Curvature$_{systole}$ [mm^{-1}]	Inferior	0.0052	[0.0040-0.0084]	0.0009	[0.0004-0.0014]	0.01
	Lateral	0.0046	[0.0033-0.0209]	0.0013	[0.0013-0.0016]	0.03
	Anterior	0.0066	[0.0051-0.0107]	0.0024	[0.0021-0.0033]	0.05
Variation Curvature$_{diastole}$ [mm^{-1}]	Inferior	0.0040	[0.0017-0.0072]	0.0007	[0.0003-0.0011]	0.01
	Lateral	0.0033	[0.0016-0.0062]	0.0010	[0.0007-0.0012]	0.01
	Anterior	0.0051	[0.0030-0.0089]	0.0021	[0.0011-0.0038]	0.01

3.4 Cyclic regional wall stresses

The left ventricle was divided into 16 segments (see figure 7) in order to asses regional left ventricular function. The wall stresses of these 16 segments during a full cardiac cycle for three

patients are depicted in figure 12. For a moment in time a map of the regional wall stress across the entire left ventricle was constructed and shown in figure 13. The wall stress for each segments for the patients group based on LVEF can be found in table 11. No significant difference between the groups were found at end-diastolic. Significant differences were found at peak systole for the segments 2, 8-11 and 13-16. At end systole a significant difference was found for segments 8. The two groups based on LVEDd showed no significant difference at end diastole. At peak systole significant differences were found for segment 2, 4, 5, 7-11 and 13-16. At end systole significant differences were found for segment 9-11 and 13-16.

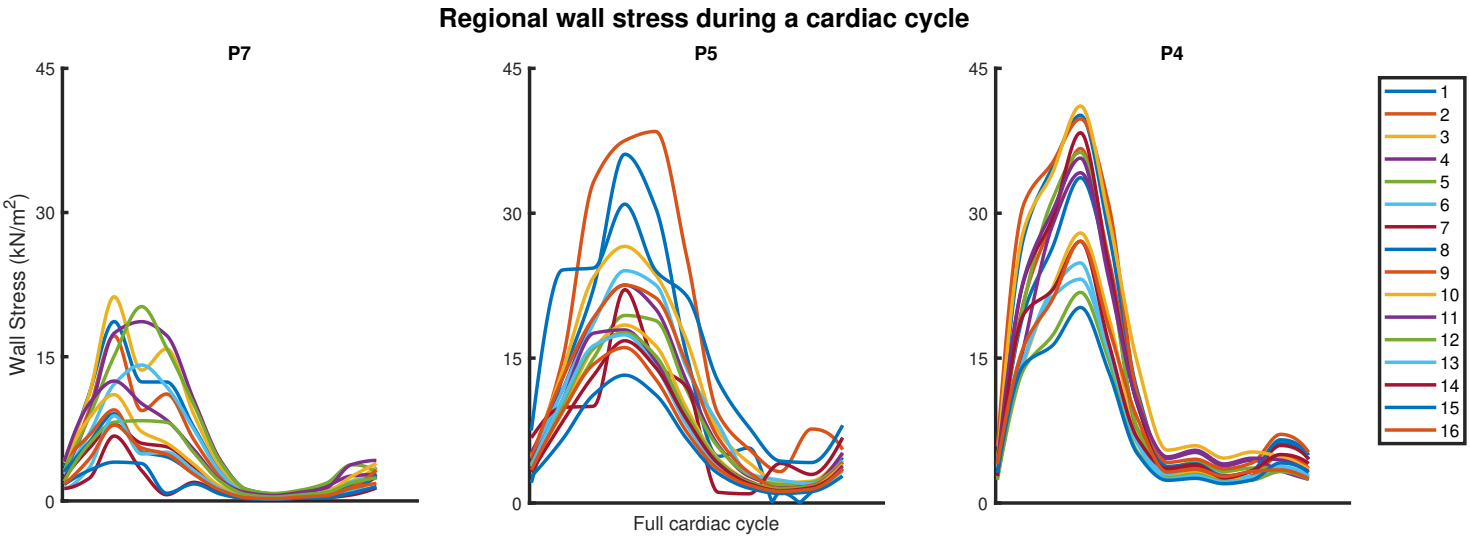

Figure 12: Regional wall stress during a cardiac cycle for three patients. Left: physiological patient, middle: HFrEF patient and right: dilated HFrEF patient.

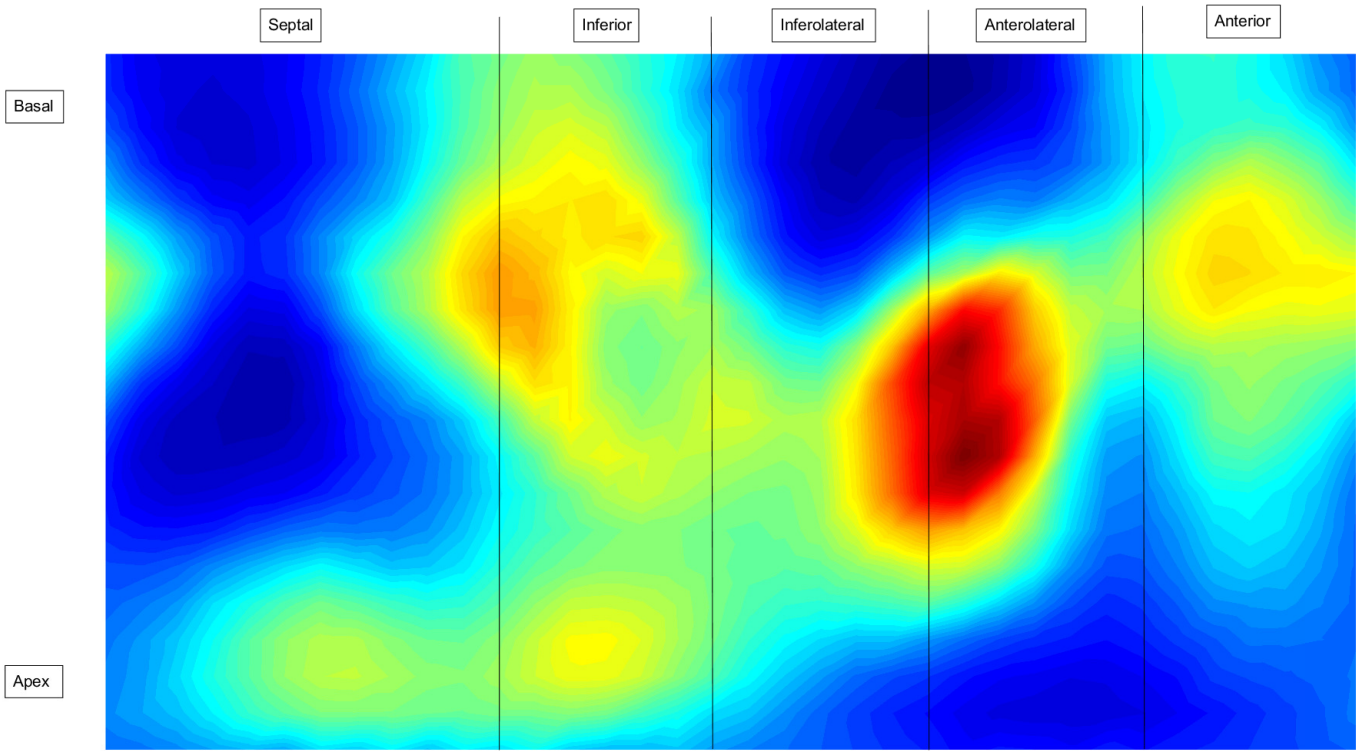

Figure 13: A map of regional wall stress over the entire left ventricle at end-diastolic for patient 4. Blue area's show low regional wall stress compared to red area's corresponding to high regional wall stresses.

Correlations between end-systolic, peak systolic and end-diastolic wall stress and wall stress change, curvature change and chance wall thickness during systole and diastole were calculated. These values are shown in table 10. Scatter plots and linear regressions for end-systolic wall stress are shown in figure 13.

Table 10: Correlations between wall stress points and change in wall stress, curvature and wall thickening during systole and diastole

	Var WS_{sys}	Var WS_{dia}	Var CR_{sys}	Var CR_{dia}	Var WT_{sys}	Var WT_{dia}	WS_{ED}	WS_{peak}
WS_{ED}	-.09	.39**	-.36**	-.50**	.11	-.41**	1.00	.38**
WS_{peak}	.80**	.33**	-.64**	-.55**	-.51**	-.32**	.38**	1.00
WS_{ES}	.30**	.86**	-.58**	-.56**	-.09	-.35**	.71**	0.65**

**Spearman's rho, significant (p <.01);
Var: variation, WS: wall stress, CR: curvature, WT: wall thickness

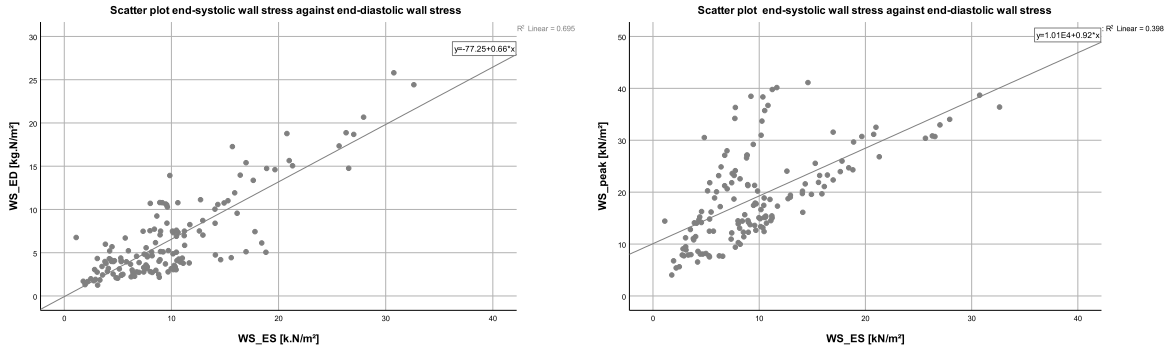

(a) End-systolic wall stress against end-diastolic wall stress.

(b) End-systolic wall stress against end-diastolic wall stress.

Figure 14: Scatter plot with linear regression for end-systolic wall stress

Table 11: end-diastolic, peak systolic and end sytolic wall stress across 16 anatomical segments

	Physiological n = 5						HFrEF n = 4								
	WS ED [kN/m2]		WS peak [kN/m2]		WS ES [kN/m2]		WS ED [kN/m2]		WS peak [kN/m2]		WS ES [kN/m2]		p-value ED	p-value peak	p-value ES
1.	6.1	[3.0-11.0]	26.0	[21.7-28.7]	17.8	[8.2-19.0]	8.7	[2.5-19.0]	32.1	[22.8-33.9]	17.1	[6.1-27.0]	1.00	0.22	0.62
2.	5.6	[3.7-14.5]	23.2	[19.5-28.2]	15.6	[7.0-19.3]	11.9	[4.2-18.8]	34.8	[31.4-38.0]	25.8	[13.2-26.8]	0.46	0.03	0.09
3.	5.0	[3.9-10.9]	24.3	[20.4-27.4]	14.9	[9.2-17.0]	6.5	[3.3-11.0]	21.6	[17.9-26.9]	13.8	[8.5-18.4]	1.00	0.46	0.81
4.	3.4	[2.9-9.5]	17.5	[13.1-22.9]	9.7	[8.7-12.4]	8.2	[3.7-16.9]	25.6	[19.1-33.4]	16.7	[7.7-23.8]	0.22	0.14	0.33
5.	3.8	[3.2-7.2]	15.6	[14.8-19.8]	9.7	[8.0-10.5]	6.0	[4.1-13.4]	25.2	[15.9-35.1]	13.5	[6.9-22.5]	0.22	0.22	0.33
6.	4.3	[2.9-8.0]	21.4	[13.1-26.7]	10.2	[8.2-13.8]	7.7	[3.2-14.0]	23.7	[17.0-26.3]	13.0	[8.8-19.8]	0.62	0.33	0.46
7.	6.9	[2.5-10.4]	16.2	[10.9-19.3]	8.0	[4.5-12.3]	7.1	[4.1-12.9]	22.9	[14.6-36.4]	17.8	[3.6-26.0]	0.62	0.33	0.33
8.	7.0	[2.6-13.8]	19.4	[13.5-25.2]	9.6	[5.8-14.3]	8.5	[4.7-20.7]	30.2	[21.8-39.2]	22.0	[13.5-31.5]	0.46	0.09	0.05
9.	4.7	[4.1-10.7]	16.1	[11.6-19.0]	9.1	[5.0-11.8]	7.1	[4.9-12.6]	22.3	[20.5-35.7]	15.2	[8.6-27.2]	0.46	0.03	0.22
10.	4.0	[3.0-7.6]	14.2	[12.1-14.3]	8.4	[4.2-9.7]	5.9	[4.0-21.3]	27.5	[15.4-40.5]	19.9	[6.0-30.4]	0.33	0.01	0.09
11.	4.1	[2.8-6.8]	11.4	[10.6-12.4]	7.4	[4.7-8.3]	5.6	[4.1-12.8]	22.5	[14.9-34.2]	15.0	[6.0-22.1]	0.22	0.01	0.14
12.	4.4	[2.2-7.8]	14.8	[10.6-19.9]	8.2	[5.2-10.3]	5.5	[2.8-7.3]	15.3	[14.7-20.2]	9.8	[5.5-13.7]	0.81	0.46	0.62
13.	2.2	[1.5-4.9]	8.1	[6.6-8.5]	4.5	[2.6-5.5]	4.2	[3.7-6.7]	15.4	[10.6-21.5]	9.0	[4.9-14.2]	0.22	0.01	0.09
14.	2.3	[1.6-4.6]	7.7	[7.1-8.2]	4.2	[2.6-5.9]	4.1	[2.9-14.3]	20.6	[12.8-29.6]	13.5	[5.7-23.4]	0.22	0.01	0.09
15.	2.7	[1.8-5.1]	7.7	[5.3-10.4]	3.8	[2.3-6.2]	4.1	[2.8-6.9]	13.4	[11.5-18.8]	8.5	4.3-12.4]	0.22	0.01	0.14
16.	3.0	[1.9-5.5]	7.9	[6.7-11.9]	5.3	[2.6-7.1]	4.4	[3.6-7.8]	16.2	[12.9-25.1]	11.5	[5.2-16.8]	0.22	0.01	0.09

WS: wall stress, ED: end-diastolic, peak: peak systolic, ES: end-systolic

3.5 Observer reliability

3.5.1 Intraobserver reliability

A two-way mixed intraclass correlation (ICC) was used to asses intraobserver reliability on the segmentation of the left ventricle during a single cardiac cycle. The ICC showed to be 0.81 across all segments and time. The ICC per segment is shown in table 12. An average of wall stress across the 16 segments over time obtained using the segmentation of the left ventricle by one observer for two times is shown in figure 15(a).

Table 12: Intraclass Correlation Coefficient for intra observer reliability

Segment	1	2	3	4	5	6	7	8	9	10	11	12	13	14	15	16
ICC	0.91	0.90	0.85	0.59	0.62	0.81	0.99	0.95	0.89	0.86	0.95	0.99	0.96	0.95	0.96	0.92

ICC: intraclass correlation coefficient

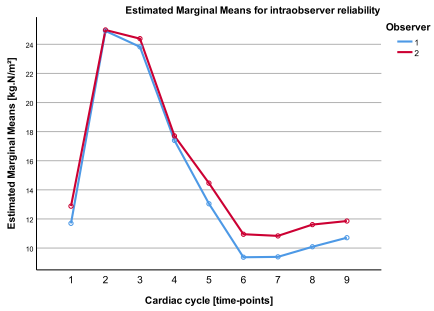

(a) Estimated marginal means for intraobserver reliability

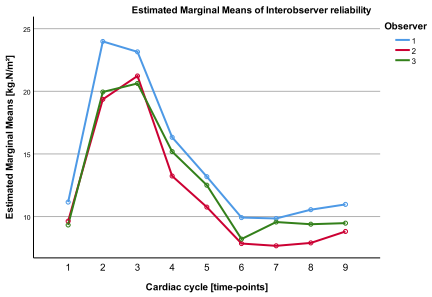

(b) Estimated marginal means for interobserver reliability

Figure 15: Intraobserver reliability

3.5.2 Interobserver reliability

Also a two-way mixed intraclass correlation (ICC) was used to asses the inter observer reliability on the segmentation of the left ventricle during a single cardiac cycle. The ICC showed to be 0.76 across all segments and time. The ICC per segment is shown in table 13. An average of wall stress across the 16 segments over time obtained using the segmentation of the left ventricle by three observers is shown in figure 15(b).

Table 13: Intraclass Correlation Coefficient for inter observer reliability

Segment	1	2	3	4	5	6	7	8	9	10	11	12	13	14	15	16
ICC	0.93	0.83	0.93	0.55	0.76	0.78	0.95	0.95	0.77	0.82	0.88	0.97	0.97	0.93	0.90	0.91

ICC: intraclass correlation coefficient

4 Discussion

This exploratory case-control pilot study focuses on quantifying the full cardiac cycle regional myocardial wall stress in patients undergoing surgery. This in order to observe for changes in regional wall stress between patients with a physiological function left ventricle and heart failure patients. With this information, possibly, an epicardial device could be developed to reduce wall stress and increase ejection fraction to improve patients outcome. This study proofs the feasibility of using three-dimensional echocardiography for obtaining the regional wall stress.

The results of the global end-diastolic and end-systolic wall stress show to be in line with previously obtained global wall stress using an ellipsoid model [35]. Peak systolic wall stress, however, is much lower for the physiological and HFrEF as calculated in this study compared to the previously obtained peak systolic wall stress. In earlier studies calculations of global wall stress were performed at the equator of the ventricle. As this is the location thought to be subjected to the highest wall stress it is logical that the peak wall stress values obtained in the current study are lower, since it is calculated as an average of the regional wall stress. Results of the comparison of global wall stress, curvature and sphericity between four patients groups show no significant differences. Although not significant there seems to be an increase in global wall stress between the physiological and dilated HFrEF group, which matches previous research as described in the introduction. The lack of significance could be explained by the low amount of patients in each group, as will be elaborated later on. Table 4 shows the average left ventricular curvature. The lower the curvature the higher the average radius of the ventricle. It can be observed, although not significant, that the curvature of the physiological and HFmrEF left ventricle is higher than that of the (dilated) HFrEF patients. This in line with the fact that in a dilated ventricle the radius is increased due to an enlargement of the ventricle. Furthermore, in HFrEF patients the radius is also increased due to a volume overload in the left ventricle. The change in curvature between end-diastolic and end-systolic also seems to be different in physiological and (dilated) HFrEF patients. Since the myocardial vitality is decreased in HFrEF patients it is explainable that the change in shape of the left ventricle is impaired. The same effect for curvature seems also applicable for the sphericity of the ventricle.

To observe which wall is effected the most by a change in pump function and ventricular shape the average wall stress per wall was determined. The septal wall was excluded from analysis since the to be developed epicardial device only could support the outside wall of the ventricle. Only a significant difference was found in peak systolic wall stress in the lateral wall based on the comparison according to LVEF. When the groups are based on the LVEDd (52mm) also at end systole a significant difference was found for the lateral and inferior wall. This suggest that the lateral and inferior wall of the ventricle is effected the most in HFrEF patients. The difference in curvature between the two groups showed to be significant for each wall at each point in time. This shows that the dilatation of the left ventricle occurs in every wall of the left ventricle. No significant differences were found for the variation in wall stress during systole and diastole between the groups. This shows that the change in rate of wall stress during a cardiac cycle is not affected. The significant differences in change of rate in curvature between the groups show that the change in curvature is affected by an impaired pump function.

The results of the regional wall stresses at end systole are in line with earlier research [27]. The results show that the wall stress is the highest for the basal segments (1-6). Wall stress is the lowest for the apical segments (13-16). Significant differences where found between patients with a physiological functioning ventricle and HFrEF patients. Comparison based on LVEF show a significant difference in wall stress for the segments 8-16 (except segment 12) at peak systole. For the comparison based on LVEDd more segments at peak systole show to be different between the two groups (table 17). Also for the two groups based on LVEDd the end systole wall stresses in segment 10-16 (except 12) show to be significantly different. These results suggest that increases in regional wall stress occur in the middle and lower parts of the ventricle, although higher wall stresses are present for the basal (upper) segments. Previous research found that dilatation of the left ventricle is present more at the middle and lower part of the left ventricle. This is in line with the findings in the current study, wall stress is increased in the middle and lower part of the ventricle. Contradictory, the wall stress is highest in the upper part of the ventricle, so one would expect that dilatation would mostly occur at the basal part of the ventricle. Why the opposite is happening could be explained by the orientation of

the muscle fibers of the ventricle. Torrent-Guasp described that the left ventricle muscle fibers are orientated in a helical way (see figure 16). The left ventricle is formed by muscle fibers oriented in a double helix. At the basal part of the ventricle an extra layer of muscle fibers is orientated circular around the ventricle. Due to the circular orientation of the fibers at the basal part it can handle stronger forces than when orientated differently. Therefore, a dilatation would be expected at the lower parts of the ventricle.

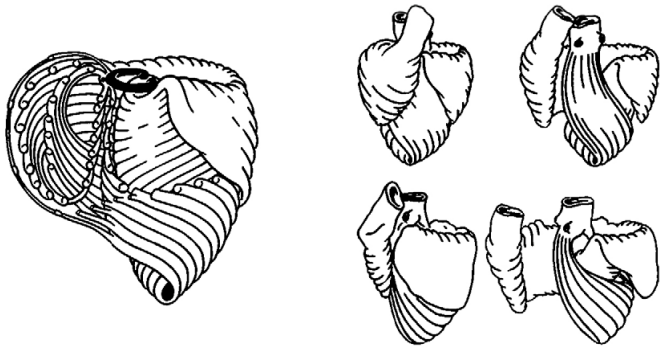

Figure 16: Myocardial band according to Torrent-Guasp. It depicts the orientation of muscle fibers of the heart [47].

Strong correlations were found between end-systolic wall stress and peak and end-diastolic wall stress, respectively 0.65 and 0.71. Knowing the end-systolic wall stress for a segment, the peak and end-diastolic wall stress could be estimated using (y = 10100+0.92x) and (y = 77.25+0.66x). R-squared, however, is less strong for the linear fitting of peak systolic wall stress ($R^2 = 0.40$) than for end-diastolic wall stress ($R^2 = 0.70$). Thus, peak systolic wall stress can be estimated less accurate. As furthermore can be observed in figure 12, when the wall stress in a segments is high at end-systole, as compared to other segments, the wall stress was remaining high during contraction. For end-diastolic wall stress the correlation with peak systolic wall stress is weak. This suggests that end-systolic wall stress is a better predictor of wall stress during a cardiac cycle. Negative moderate correlations were found between wall stress and change in curvature during systole and diastole. This confirms that higher wall stresses are accompanied with a less functioning ventricle. No significant correlations were found between end-systolic and end-diastolic wall stress and change in wall thickness during systole. Peak systolic wall stress is moderately negative correlated with the change in wall thickness during systole and diastole. This suggest that peak systolic wall stress is an indicator of muscle vitality.

4.1 Limitations

As this is an explorational study only 11 patients were included. In total 9 patients were eligible for analysis. Although this gave a good insight into the differences of regional wall stress, curvature and ventricle function between individual patients, conclusions between different patients groups must be drawn with caution. A lack of significant differences could for instance be explained by a low amount of included patients. More patients are needed to be analysed in order to confirm the found correlations and differences and to see if other significant differences could be found. Another factor of influence is the definition of constructed patient groups. Using the criteria LVEF and LVEDd a group with a physiological functioning ventricle was defined. Questions were raised whether this group really had a physiological functioning ventricle. As these patients had to undergo cardiac surgery it could be expected that some mall functions in the left ventricle could occur. Local ischemia, for instance, could alter the local myocardial function. Although pump function is still found physiological (LVEF > 45%), local variations

in functioning could be present affecting the results in the research. It is thought that when including more patients these local effects could be neglected.

Another limitation is that measurements were performed during surgery. It was proven that the use of anesthetics could affect the blood pressure and cardiac contractility [48]. Thus affecting the determination of regional wall stress. As measurements were conducted when a patient was under anesthesia the results in the current study could be different than in physiological conditions.

The use of TEE for the quantification of curvature and wall thickness brings another limitation. Occurring artefacts during measurements could likely affect the contouring of the endocardial and epicardial contour. Acoustic shadowing sometimes occurred due to tissue with a large attenuation coefficient. For instance, shadowing caused by calcified aortic or mitral valves. For the increase in temporal resolution the 6-beats-mode of the ultrasound device was used. It averages 6, ECG-gated, single heart beats into one heart beat, so that more frames per second of the cardiac cycle were available. However, in patients with an irregular ECG interval sometimes stitching artefacts occurred. This means that at some locations of the image the myocardium was represented irregular. This forced the observer to make estimations of the myocardial contour on that particular location, possibly inducing inaccuracies in curvature and wall thickness calculations. Imaging of the entire left ventricle using TEE proved to be difficult sometimes. One patient, for instance, was excluded from analysis because echo graphic recordings of the entire left ventricle appeared to have failed. TEE is dependent on the orientation of the heart in relation to the esophagus to be able to capture the entire left ventricle. When a heart, for instance, is rotated or moved due to a ventricular aneurysm imaging of the ventricle could be impaired. For these patient epicardial echocardiography could be used during surgery to overcome the limitation. Using epicardial echocardiography one is able to place the probe directly on the left ventricle and is not dependent on the orientation of the heart. Another example of the limitation as described above, could be observed in the results of patient 2 (figure 10). These results show to be notable different. Wall stress throughout the cardiac appeared to be high and following a different pattern than the other patients. It could be that the TEE measurement was influenced negatively due to artefacts. Also an error in pressure measurements could explain the high wall stresses. This should also be taken into account when interpreting the results and making conclusions.

Intraclass correlations show that multiple observers agree on contouring the endocardial and epicardial border. However, still some user dependent variations could be induced. This could be for instance be observed for segment 4 with an ICC of 0.55. Furthermore, only one patient was used to observe for observer reliability. Including more patients in the reliability analysis results could be different. Using an automatic segmentation method the inter-observer variability could be reduced. Furhtermore, manual segmentation of the left ventricle showed to be very labour intensive. Therefore only segmentation for a defined set of frames was performed (13 frames per second). This could influence the determination of the cyclic regional wall stress. It is possible that certain patterns in cyclic regional wall stress could be unnoticed.

For the calculation of the normal stress in the current study it was assumed that radius was sufficiently larger than the wall thickness. However this is not the case. No variations in wall stress from endocardium to epicardium could be determined. Furthermore, shear stress was neglected in the current method. These effects are physiologically significant for the left ventricle. For obtaining the average regional wall stress in the myocardium it was found that using the Laplace analysis is valid to employ. Since the goal is to eventually develop a device employed around the epicardium for lowering regional wall stress it is thought thought to be sufficient to asses the average wall stress with Laplace's law. The myocardial fiber orientation was neglected in calculating the regional wall stress. As described above the fiber orientation is of importance to determine the final effect of ventricle dilatation and impaired pump function

on the stress in the myocardium.

4.2 Clinical relevance

This study shows that regional wall stresses are increased throughout the cardiac cycle for HFrEF patients. Furthermore, it shows that when the end-systolic wall stress is obtained, end-diastolic wall stress could be determined. This study is of clinical relevance in providing knowledge into when cyclic regional wall stresses are increased. Measurement of the regional wall stress in clinical practice can therefore be used to monitor whether treatment of HFrEF patients is beneficial in the reduction of regional wall stress. This could prevent further dilatation and worsening of heart failure. The found relationship between end-systolic wall stress and end-diastolic wall stress is of great use. As only measuring end-systolic wall stress is sufficient to obtain the end-diastolic regional wall stress it could be measured non-invasivly. End-systolic wall stress could be obtained using a pressure cuff, as a surrogate for the pressure in the ventricle at end systole [49]. The curvature and wall thickness could be determined with three-dimensional echocardiography or MRI measurements simultaneously. MRI will improve the quality of measurements, however it comes with the downside that it is more invasive than using echo. The end-diastolic stresses could than be estimated using the found relationship. Peak systolic wall stress could also be estimated using the found relationship, however, it is less accurate. This relationship could be of use to non-invasivly monitor the regional wall stress in HFrEF patients over a period of time which would be beneficial as described above.

4.3 Future device properties

Based on the results a theoretical cardiac device for lowering the regional wall stress and improving ejection fraction could be described. As observed, regional wall stress in the lower parts of the ventricle is increased during systole in HFrEF patients. A device surrounding the outside of the left ventricle could be used to lower these wall stresses. Based on the correlation between end-diastolic regional wall stress and end-systolic regional wall stress and previous developed devices it is thought that lowering the end-diastolic wall stress, the wall stress throughout the cardiac cycle could be lowered. This could be performed by epicardially surrounding the left ventricle with a rigid sleeve which prevents overfilling of the left ventricle and reducing end-diastolic volume. When end-diastolic volume is decreased, ejection fraction is increased [50]. Due to a smaller dimension of the ventricle wall stresses are lower throughout the cardiac cycle. This is in line with previous epicardial devices developed as described in section 1.5. Subsequently, it is thought that wall stress throughout the cardiac cycle is needed to be decreased further using active support. As observed, peak systolic wall stresses in dilated ventricle are approximately two times higher than in a physiological function ventricle. It was furthermore found that myocardial vitality is decreased, and thus the ability to contract, when peak systolic is increased. When an epicardial device could contract, and thus become smaller, during systole it could substitute the myocardium with lost vitality and increase the curvature of the ventricle even more. This could lower the peak systolic wall stress even more. It is thought that the amount of active support could be different for different locations of the ventricle. Locations with a higher increased regional wall stress are needed to be supported more actively. So, a patient specific device is recommended. As myocardial reverse remodelling occurs when lowering the wall stress one should assess the regional function and wall stress in follow-up to make adjustments in the settings of active support.

Lowering the end-diastolic volume could be performed by a passive rigid sleeve around the left ventricle. Materials such as PTFE and Dacron are suitable as they are proven to be rigid and safely implantable [51]. For the active part shape memory alloys could, for instance, be

used as they are relatively small and thus could be minimally invasive deployed. A shape memory alloy, for instance flexinol, can contract when applying a current. It is proven feasible to use flexinol to improve ejection fraction [52]. However, still some challenges, such as heat production and energy usage are needed to be overcome in order to used in patients. The device should furthermore be able to operate without any per-cutaneous line as they promote infections and it is desirable that the device can be implemented minimal invasively.

4.4 Recommendations

This research could be used as a basis for further research. For further research some recommendations could be made. As already mentioned segmentation, of the left ventricle in the current study depends on the interpretation of the observer. Automatic segmentation of the left ventricle would improve the quality of segmentation and will reduce any variability in segmentation between patients. Furthermore, it would make the segmentation time much shorter and it would decrease manual labour massively. Therefore it would be possible to segment the left ventricle for every point in time. Fully automatic segmentation of the endocardial and epicardial contour in three-dimensional echo is still under development. Due to the lower spatial resolution, speckle, possible introduction of acoustic shadowing and stitching artefacts fully automatic segmentation is difficult. A method developed by Pedrosa et al. is capable of segmenting both the endocardial and epicardoial contour [53]. This method could be used in further research to improve the quality of segmentation and reduce segmentation time.

Further research should also include a comparison between regional wall stress assessed with echocardiograhy and MRI. Since MRI has a higher spatial resolution a more precise calculation of regional wall stresses could be performed. Furthermore, MRI has a higher temporal resolution, thus more frames within a cardiac cycle could be assessed. MRI coupled with late gadolinium enhancement (LGE) adds useful information of local ischemia and infarction. Further research should determine in what extend echocardiographic imaging is comparable with MRI. This in order to be able to use echography to assess regional wall stress in clinical practice.

As already mentioned, the current study included a low amount of patients. Further research should include more patients to be able to draw stronger conclusions. Furthermore, including more patients makes it possible to differentiate patients into more groups to be able to compare different disease etiologies and its consequence on cyclic regional wall stress. Furthermore, a further differentiation based on LVEF should be made. As LVEF is a predictor for survival in HFrEF patients it is of use to asses the cyclic regional wall stress for incremental steps in LVEF (10,15...40,45%). This in order to observe for a possible relation between LVEF and wall stress for heart failure patients with different pump function. Furthermore, this would give insight into the amount of wall stress needed to be reduced for an increase in survival. This analysis was not possible in the current study since HFrEF patients only had LVEF between 32 and 36%. Also longitudinal research into the regional wall stress is recommended. This could provide information of the effect of (pharmacological) treatment onto regional wall stress.

To be able to describe the geometry of the left ventricle more accurately the use of a finite element model (FEM) is required. This method could furthermore include nonlinear and anisotropic material properties, myocardial fibre orientation and myocardial strain in the calculation for regional wall stress. This would provide a better insight into the regional wall stresses during diastole and systole and into the influence of the myocardial fiber orientation on left ventricular dilatation, since myocardial fiber orientation is neglected in the current study [35].

5 Conclusion

Full cardiac cycle left ventricular regional wall stress was successfully quantified during cardiac surgery with the use of three-dimensional echocardiography and left ventricular pressure recordings. The current study gives insight into the differences in regional wall stress between physiological function left ventricles and impaired and dilated ventricles. Regional wall stress for the middle and apical segments of the ventricle for HFrEF patients with a dilated ventricle are found to be increased at peak systole and end-systole. Correlations were found between end-systolic wall stress and peak systolic and end-diastolic wall stress. Peak systolic wall stress shows to be moderately negatively correlated with the change in curvature and change in wall thickness during systole and diastole. This suggests that peak systolic wall stress is an indicator for muscle vitality.

The current study provides insight into for which segments regional wall stresses during a cardiac cycle are needed to be lowered. It suggests that peak systolic wall stresses are needed to be lowered for the middle and apical part of the left ventricle.

This study is a good first step and offers a basis for further research. Future work should focus on changes in regional wall over time after treatment and the relationship between different LVEF. Furthermore, it should focus on developing a minimal invasive device with patient-specific full cardiac cycle support in order to lower regional wall stress.

References

[1] P. Ponikowski, A. A. Voors, S. D. Anker, H. Bueno, J. G. Cleland, A. J. Coats, V. Falk, J. R. González-Juanatey, V.-P. Harjola, E. A. Jankowska, *et al.*, "2016 esc guidelines for the diagnosis and treatment of acute and chronic heart failure: The task force for the diagnosis and treatment of acute and chronic heart failure of the european society of cardiology (esc). developed with the special contribution of the heart failure association (hfa) of the esc," *European journal of heart failure*, vol. 18, no. 8, pp. 891–975, 2016.

[2] V. L. Roger, "Epidemiology of heart failure," *Circulation research*, vol. 113, no. 6, pp. 646–659, 2013.

[3] E. J. Benjamin, S. S. Virani, C. W. Callaway, A. M. Chamberlain, A. R. Chang, S. Cheng, S. E. Chiuve, M. Cushman, F. N. Delling, R. Deo, *et al.*, "Heart disease and stroke statistics—2018 update: a report from the american heart association," *Circulation*, vol. 137, no. 12, pp. e67–e492, 2018.

[4] D. M. Henkel, M. M. Redfield, S. A. Weston, Y. Gerber, and V. L. Roger, "Death in heart failure: a community perspective," *Circulation: Heart Failure*, vol. 1, no. 2, pp. 91–97, 2008.

[5] J. Duchenne, "Improving heart failure morbidity through individually tailored disease management," Master's thesis, tUL, 2013.

[6] R. S. Vasan, M. G. Larson, E. J. Benjamin, J. C. Evans, C. K. Reiss, and D. Levy, "Congestive heart failure in subjects with normal versus reduced left ventricular ejection fraction: prevalence and mortality in a population-based cohort," *Journal of the American College of Cardiology*, vol. 33, no. 7, pp. 1948–1955, 1999.

[7] G. L. Smith, F. A. Masoudi, V. Vaccarino, M. J. Radford, and H. M. Krumholz, "Outcomes in heart failure patients with preserved ejection fraction: mortality, readmission, and functional decline," *Journal of the American College of Cardiology*, vol. 41, no. 9, pp. 1510–1518, 2003.

[8] F. Pons, J. Lupón, A. Urrutia, B. González, E. Crespo, C. Díez, L. Cano, R. Cabanes, S. Altimir, R. Coll, *et al.*, "Mortality and cause of death in patients with heart failure: findings at a specialist multidisciplinary heart failure unit," *Revista Española de Cardiología (English Edition)*, vol. 63, no. 3, pp. 303–314, 2010.

[9] M. analysis Global Group in Chronic Heart Failure (MAGGIC), "The survival of patients with heart failure with preserved or reduced left ventricular ejection fraction: an individual patient data meta-analysis," *European Heart Journal*, vol. 33, no. 14, pp. 1750–1757, 2011.

[10] O. Chioncel, M. Lainscak, P. M. Seferovic, S. D. Anker, M. G. Crespo-Leiro, V.-P. Harjola, J. Parissis, C. Laroche, M. F. Piepoli, C. Fonseca, *et al.*, "Epidemiology and one-year outcomes in patients with chronic heart failure and preserved, mid-range and reduced ejection fraction: an analysis of the esc heart failure long-term registry," *European journal of heart failure*, vol. 19, no. 12, pp. 1574–1585, 2017.

[11] M. R. MacDonald, P. P. Wee, Y. Cao, D. M. Yang, S. Lee, K. L. Tong, and K. T. G. Leong, "Comparison of characteristics and outcomes of heart failure patients with preserved versus reduced ejection fraction in a multiethnic southeast asian cohort," *The American journal of cardiology*, vol. 118, no. 8, pp. 1233–1238, 2016.

[12] K. S. Shah, H. Xu, R. A. Matsouaka, D. L. Bhatt, P. A. Heidenreich, A. F. Hernandez, A. D. Devore, C. W. Yancy, and G. C. Fonarow, "Heart failure with preserved, borderline, and reduced ejection fraction: 5-year outcomes," *Journal of the American College of Cardiology*, vol. 70, no. 20, pp. 2476–2486, 2017.

[13] J. P. Curtis, S. I. Sokol, Y. Wang, S. S. Rathore, D. T. Ko, F. Jadbabaie, E. L. Portnay, S. J. Marshalko, M. J. Radford, and H. M. Krumholz, "The association of left ventricular ejection fraction, mortality, and cause of death in stable outpatients with heart failure," *Journal of the American College of Cardiology*, vol. 42, no. 4, pp. 736–742, 2003.

[14] S. J. Pocock, D. Wang, M. A. Pfeffer, S. Yusuf, J. J. McMurray, K. B. Swedberg, J. Ostergren, E. L. Michelson, K. S. Pieper, and C. B. Granger, "Predictors of mortality and morbidity in patients with chronic heart failure," *European heart journal*, vol. 27, no. 1, pp. 65–75, 2005.

[15] J. Lupon, C. Díez-López, M. de Antonio, M. Domingo, E. Zamora, P. Moliner, B. Gonzalez, J. Santesmases, M. I. Troya, and A. Bayés-Genís, "Recovered heart failure with reduced ejection fraction and outcomes: a prospective study," *European journal of heart failure*, vol. 19, no. 12, pp. 1615–1623, 2017.

[16] J. Lupón, G. Gavidia-Bovadilla, E. Ferrer, M. de Antonio, A. Perera-Lluna, J. López-Ayerbe, M. Domingo, J. Núñez, E. Zamora, P. Moliner, *et al.*, "Dynamic trajectories of left ventricular ejection fraction in heart failure," *Journal of the American College of Cardiology*, vol. 72, no. 6, pp. 591–601, 2018.

[17] J. G. Cleland, J.-C. Daubert, E. Erdmann, N. Freemantle, D. Gras, L. Kappenberger, and L. Tavazzi, "Longer-term effects of cardiac resynchronization therapy on mortality in heart failure [the cardiac resynchronization-heart failure (care-hf) trial extension phase]," *European heart journal*, vol. 27, no. 16, pp. 1928–1932, 2006.

[18] K. V. Burns, R. M. Gage, A. E. Curtin, and A. J. Bank, "Long-term echocardiographic response to cardiac resynchronization therapy in initial nonresponders," *JACC: Heart Failure*, vol. 3, no. 12, pp. 990–997, 2015.

[19] E. D. Walter and R. Hetzer, "Surgical treatment concepts for heart failure," *HSR proceedings in intensive care & cardiovascular anesthesia*, vol. 5, no. 2, p. 69, 2013.

[20] C. Murphy, H. Zafar, and F. Sharif, "An updated review of cardiac devices in heart failure," *Irish Journal of Medical Science (1971-)*, vol. 186, no. 4, pp. 909–919, 2017.

[21] D. Shchekochikhin, F. Al Ammary, J. A. Lindenfeld, and R. Schrier, "Role of diuretics and ultrafiltration in congestive heart failure," *Pharmaceuticals*, vol. 6, no. 7, pp. 851–866, 2013.

[22] J. L. Hellawell and K. B. Margulies, "Myocardial reverse remodeling," *Cardiovascular therapeutics*, vol. 30, no. 3, pp. 172–181, 2012.

[23] P. Alter, A. R. Koczulla, C. Nell, J. H. Figiel, C. F. Vogelmeier, and M. B. Rominger, "Wall stress determines systolic and diastolic function—characteristics of heart failure," *International journal of cardiology*, vol. 202, pp. 685–693, 2016.

[24] T. Saraon and S. D. Katz, "Reverse remodeling in systolic heart failure," *Cardiology in review*, vol. 23, no. 4, pp. 173–181, 2015.

[25] W. Grossman, "Cardiac hypertrophy: useful adaptation or pathologic process?," *The American journal of medicine*, vol. 69, no. 4, pp. 576–584, 1980.

[26] D. L. Mann, "Basic mechanisms of left ventricular remodeling: the contribution of wall stress," *Journal of cardiac failure*, vol. 10, no. 6, pp. S202–S206, 2004.

[27] L. Zhong, Y. Su, S.-Y. Yeo, R.-S. Tan, D. N. Ghista, and G. Kassab, "Left ventricular regional wall curvedness and wall stress in patients with ischemic dilated cardiomyopathy," *American Journal of Physiology-Heart and Circulatory Physiology*, vol. 296, no. 3, pp. H573–H584, 2009.

[28] K.-M. Jan, "Distribution of myocardial stress and its influence on coronary blood flow," *Journal of biomechanics*, vol. 18, no. 11, pp. 815–820, 1985.

[29] J. Schwitter, F. R. Eberli, M. Ritter, M. Turina, and H. P. Krayenbuehl, "Myocardial oxygen consumption in aortic valve disease with and without left ventricular dysfunction.," *Heart*, vol. 67, no. 2, pp. 161–169, 1992.

[30] P. Di Napoli, A. A. Taccardi, A. Grilli, M. Felaco, A. Balbone, D. Angelucci, S. Gallina, A. M. Calafiore, R. De Caterina, and A. Barsotti, "Left ventricular wall stress as a direct correlate of cardiomyocyte apoptosis in patients with severe dilated cardiomyopathy," *American heart journal*, vol. 146, no. 6, pp. 1105–1111, 2003.

[31] P. Alter, H. Rupp, M. Rominger, F. Czerny, A. Vollrath, K. Klose, and B. Maisch, "A new method to assess ventricular wall stress in patients with heart failure and its relation to heart rate variability," *International journal of cardiology*, vol. 139, no. 3, pp. 301–303, 2010.

[32] W. P. Hood Jr, W. J. Thomson, C. E. RACKLEY, and E. L. ROLETT, "Comparison of calculations of left ventricular wall stress in man from thin-walled and thick-walled ellipsoidal models," *Circulation research*, vol. 24, no. 4, pp. 575–582, 1969.

[33] W. P. Hood Jr, C. E. Rackley, and E. L. Rolett, "Wall stress in the normal and hypertrophied human left ventricle," *The American journal of cardiology*, vol. 22, no. 4, pp. 550–558, 1968.

[34] H. Sandler and H. T. Dodge, "Left ventricular tension and stress in man," *Circulation research*, vol. 13, no. 2, pp. 91–104, 1963.

[35] L. Zhong, D. Ghista, and R. Tan, "Left ventricular wall stress compendium," *Computer methods in biomechanics and biomedical engineering*, vol. 15, no. 10, pp. 1015–1041, 2012.

[36] J. Oomen, S. Trines, W. Vermeulen, R. Krams, J. Schuurbiers, W. Vletter, J. Roelandt, and C. Slager, "Towards assessment of regional wall stress of the left ventricle using 3d ultrasound imaging," in *Computers in Cardiology 1999. Vol. 26 (Cat. No. 99CH37004)*, pp. 129–132, IEEE, 1999.

[37] N. Hassan, J.-M. Escanyé, Y. Juillière, P.-Y. Marie, N. David, P. Olivier, A. Ayalew, G. Karcher, J.-F. Stolz, and A. Bertrand, "201tl spect abnormalities, documented at rest in dilated cardiomyopathy, are related to a lower than normal myocardial thickness but not to an excess in myocardial wall stress," *Journal of Nuclear Medicine*, vol. 43, no. 4, pp. 451–457, 2002.

[38] N. D'Elia, J. D'hooge, and T. H. Marwick, "Association between myocardial mechanics and ischemic lv remodeling," *JACC: Cardiovascular Imaging*, vol. 8, no. 12, pp. 1430–1443, 2015.

[39] D. L. Mann, S. H. Kubo, H. N. Sabbah, R. C. Starling, M. Jessup, J. K. Oh, and M. A. Acker, "Beneficial effects of the corcap cardiac support device: five-year results from the acorn trial," *The Journal of thoracic and cardiovascular surgery*, vol. 143, no. 5, pp. 1036–1042, 2012.

[40] M. Naveed, I. S. Mohammad, L. Xue, S. Khan, W. Gang, Y. Cao, Y. Cheng, X. Cui, C. DingDing, Y. Feng, *et al.*, "The promising future of ventricular restraint therapy for the management of end-stage heart failure," *Biomedicine & Pharmacotherapy*, vol. 99, pp. 25–32, 2018.

[41] L. S. Lee, R. K. Ghanta, S. A. Mokashi, O. Coelho-Filho, R. Y. Kwong, M. Kwon, J. Guan, R. Liao, and F. Y. Chen, "Optimized ventricular restraint therapy: Adjustable restraint is superior to standard restraint in an ovine model of ischemic cardiomyopathy," *The Journal of thoracic and cardiovascular surgery*, vol. 145, no. 3, pp. 824–831, 2013.

[42] S. A. Mokashi, L. S. Lee, J. D. Schmitto, R. K. Ghanta, S. McGurk, R. G. Laurence, R. M. Bolman III, L. H. Cohn, and F. Y. Chen, "Restraint to the left ventricle alone is superior to standard restraint," *The Journal of thoracic and cardiovascular surgery*, vol. 146, no. 1, pp. 192–197, 2013.

[43] R. D. Sumanasinghe and M. W. King, "New trends in biotextiles–the challenge of tissue engineering," *J Text Apparel Technol Manage*, vol. 3, no. 2, pp. 1–13, 2003.

[44] G. C. Christensen, J. Raman, A. Kilic, and B. A. Whitson, "Ventricular containment, shape change, infarct restraint," in *Management of Heart Failure*, pp. 121–136, Springer, 2016.

[45] R. M. Lang, L. P. Badano, V. Mor-Avi, J. Afilalo, A. Armstrong, L. Ernande, F. A. Flachskampf, E. Foster, S. A. Goldstein, T. Kuznetsova, *et al.*, "Recommendations for cardiac chamber quantification by echocardiography in adults: an update from the american society of echocardiography and the european association of cardiovascular imaging," *European Heart Journal-Cardiovascular Imaging*, vol. 16, no. 3, pp. 233–271, 2015.

[46] J. Yeboah, D. A. Bluemke, W. G. Hundley, C. J. Rodriguez, J. A. Lima, and D. M. Herrington, "Left ventricular dilation and incident congestive heart failure in asymptomatic adults without cardiovascular disease: multi-ethnic study of atherosclerosis (mesa)," *Journal of cardiac failure*, vol. 20, no. 12, pp. 905–911, 2014.

[47] M. J. Kocica, A. F. Corno, F. Carreras-Costa, M. Ballester-Rodes, M. C. Moghbel, C. N. Cueva, V. Lackovic, V. I. Kanjuh, and F. Torrent-Guasp, "The helical ventricular myocardial band: global, three-dimensional, functional architecture of the ventricular myocardium," *European journal of cardio-thoracic surgery*, vol. 29, no. Supplement_1, pp. S21–S40, 2006.

[48] M. K. Loushin, "The effects of anesthetic agents on cardiac function," in *Handbook of Cardiac Anatomy, Physiology, and Devices*, pp. 171–180, Springer, 2005.

[49] N. Reichek, J. Wilson, M. St John Sutton, T. A. Plappert, S. Goldberg, and J. W. Hirshfeld, "Noninvasive determination of left ventricular end-systolic stress: validation of the method and initial application.," *Circulation*, vol. 65, no. 1, pp. 99–108, 1982.

[50] I. Palacios, E. Powers, and W. J. Powell Jr, "Effect of end-diastolic volume on the canine left ventricular ejection fraction," *American heart journal*, vol. 109, no. 5, pp. 1059–1069, 1985.

[51] C. Singh, C. S. Wong, and X. Wang, "Medical textiles as vascular implants and their success to mimic natural arteries," *Journal of functional biomaterials*, vol. 6, no. 3, pp. 500–525, 2015.

[52] K. Aarnink, F. Halfwerk, S. A. Saïd, J. Grandjean, and J. Paulusse, "Technical feasibility and design of a shape memory alloy support device to increase ejection fraction in patients with heart failure," *Cardiovascular engineering and technology*, vol. 10, no. 1, pp. 1–9, 2019.

[53] J. Pedrosa, D. Barbosa, B. Heyde, F. Schnell, A. Rösner, P. Claus, and J. D'hooge, "Left ventricular myocardial segmentation in 3-d ultrasound recordings: Effect of different endocardial and epicardial coupling strategies," *IEEE transactions on ultrasonics, ferroelectrics, and frequency control*, vol. 64, no. 3, pp. 525–536, 2016.

Appendices

A Derivation Wall Stress

The definition of stress is the force acting over a cross-sectional area of an object:

$$\sigma = \frac{F}{A_w} \tag{4}$$

Definition of stress; with σ = Stress (N/m^2), F = Force (N) and A_w = Cross-sectional area of wall (m^2)

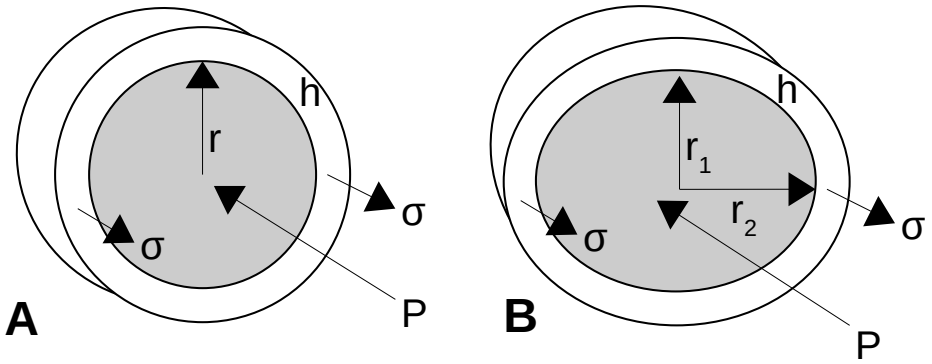

Figure 17: Schematic drawing of models and parameters to calculate wall stress. A: spherical model. B: Ellipsoidal model.

Sphere

For a sphere the normal stress can be derived as follows. First it is assumed that:

- The wall material is isotropic
- The thickness of the wall is sufficiently smaller than the radius (h<<r)

The force on the wall is described by the pressure inside the sphere acting on the wall of the sphere equally in every direction. It can be described by the pressure acting on the cross-sectional area.

$$F = P \cdot A$$
$$F = P \cdot \pi \cdot R^2 \tag{5}$$

The area of wall in the cross section is determined by:

$$A_w = A_{total} - A_{inner}$$
$$A_w = \pi \cdot (R+h)^2 - \pi \cdot R^2$$
$$A_w = \pi \cdot R^2 + \pi \cdot h^2 + 2 \cdot \pi \cdot Rh - \pi \cdot R^2 \tag{6}$$

With assumption that the radius is sufficiently greater than the thickness of the wall the term πh^2 can be neglected:

$$A_w = 2 \cdot \pi \cdot R \cdot h \tag{7}$$

Substituting both equation (5) and (7) into equation (4) the final equation for wall stress according Laplace can be derived:

$$\sigma = \frac{P \cdot \pi \cdot R^2}{2\pi \cdot R \cdot h}$$
$$\sigma = \frac{P \cdot R}{2 \cdot h} \tag{8}$$

Ellipse

The wall stress in an ellipse (spheroid) can be derived by using the maximum and minimum curvature of the ellipse and using the same assumptions determined for a spherical model. The force on the ellipsoid cross section is:

$$F = P \cdot \pi \cdot R_1 \cdot R_2 \tag{9}$$

The area of the wall of the ellipsoid cross section can be calculated using the maximum and minimum radius:

$$A_w = \pi \cdot (R_1 + h) \cdot (R_2 + h) - \pi \cdot R_1 \cdot R_2$$
$$A_w = \pi \cdot R_1 \cdot R_2 + \pi \cdot R_1 \cdot h + \pi \cdot R_2 \cdot h + \pi \cdot h^2 - \pi \cdot R_1 \cdot R_2 \tag{10}$$

Again using h << R:

$$A_w = \pi \cdot R_1 \cdot h + \pi \cdot R_2 \cdot h$$
$$A_w = \pi \cdot h \cdot (R_1 + R_2) \tag{11}$$

Substituting equation (9) an (11) into equation (4) and simplification provides the equation for wall stress in an ellipse:

$$\sigma = \frac{P \cdot \pi \cdot R_1 \cdot R_2}{\pi \cdot h \cdot (R_1 + R_2)}$$
$$\sigma = \frac{P \cdot \pi \cdot R_1 \cdot R_2}{\pi \cdot h \cdot (R_1 + R_2)} \cdot \frac{\frac{1}{R_1} \cdot \frac{1}{R_2}}{\frac{1}{R_1} \cdot \frac{1}{R_2}}$$
$$\sigma = \frac{P}{\frac{h \cdot R_1}{R_1 \cdot R2} + \frac{h \cdot R_2}{R_1 \cdot R2}}$$
$$\sigma = \frac{P}{h \cdot (\frac{1}{R_1} + \frac{1}{R_2})} = \frac{P}{h \cdot (\kappa_1 + \kappa_2)} \tag{12}$$

B Additional tables

Table 14: p-values of comparison of global paramaters, Wall Stress, Curvature and Sphericity between the four patient groups. The top row of the table depicts the two groups compared with each other.

	Physiological HFmrEF	Physiological HFrEF	Physiological Dilated HFrEF	HFmrEF HFrEF	HFmrEF Dilated HFrEF	HFrEF Dilated HFrEF
WS_{ED}	0.80	1.00	0.80	0.67	1.00	1.00
WS_{peak}	0.80	0.36	0.13	0.67	0.67	0.33
WS_{ES}	0.80	1.00	0.13	1.00	0.67	0.33
$Curvature_{ED}$	0.80	0.13	0.13	0.67	0.67	0.12
$Curvature_{peak}$	0.80	0.13	0.13	0.67	0.67	0.12
$Curvature_{ES}$	1.00	0.13	0.13	0.67	0.67	0.12
$Sphericity_{ED}$	0.80	0.13	0.13	0.67	0.67	0.12
$Sphericity_{peak}$	1.00	0.13	0.13	0.67	0.67	0.12
$Sphericity_{ES}$	0.80	0.13	0.13	0.67	0.67	0.12
ΔCurvature	1.00	0.27	0.13	0.67	0.67	1.00
ΔSphericity	0.40	0.13	0.13	0.67	0.67	1.00

WS: wall stress, ED: end-diastolic, peak: peak systolic, ES: end-systolic

Table 15: p-values of comparison of wall stress and curvature across different outside walls of the left ventricle during a cardiac cycle. Based on the comparison of two groups (LVEDd < 52mm (n=6) and LVEDd > 52mm (n=3)).

		p-value WS	p-value Curvature
	Inferior	0.30	0.02
End-diastolic	Lateral	0.20	0.04
	Anterior	0.44	0.07
	Inferior	0.44	0.02
Peak systolic	Lateral	0.04	0.07
	Anterior	0.12	0.07
	Inferior	0.04	0.02
End-systolic	Lateral	0.02	0.02
	Anterior	0.07	0.04

Table 16: p-values of comparison of variation in wall stress and curvature across different outside walls of the left ventricle during systole and diastole. Based on the comparison of two groups (LVEDd < 52mm (n=6) and LVEDd > 52mm (n=3)).

		p-value WS	p-value Curvature
	Inferior	0.80	0.02
Variation systole	Lateral	0.44	0.04
	Anterior	0.61	0.04
	Inferior	1.00	0.02
Variation diastole	Lateral	0.61	0.07
	Anterior	0.61	0.02

Table 17: p-values of comparison of regional wall stress. Based on the comparison of two groups (LVEDd < 52mm (n=6) and LVEDd > 52mm (n=3)).

	p-value ED	p-value peak	p-value ES
1.	0.30	0.12	0.30
2.	0.30	0.02	0.20
3.	0.80	0.20	0.44
4.	0.20	0.04	0.12
5.	0.12	0.04	0.30
6.	0.61	0.12	0.44
7.	0.44	0.04	0.12
8.	0.44	0.02	0.12
9.	0.20	0.04	0.07
10.	0.12	0.02	0.04
11.	0.20	0.02	0.02
12.	0.61	0.12	0.44
13.	0.20	0.02	0.04
14.	0.20	0.02	0.04
15.	0.12	0.04	0.02
16.	0.12	0.02	0.02